Uncertainty and Sensitivity Analysis of a Fire-Induced Accident Scenario involving Binary Variables and Mechanistic Codes

By

Mark A. Minton
Lieutenant, United States Navy

B.S. Nuclear Engineering, 2001
Oregon State University

Master of Engineering Management, 2008
Old Dominion University

SUBMITTED TO THE DEPARTMENT OF NUCLEAR SCIENCE AND ENGINEERING IN PARTIAL FULFILLMENT OF THE REQUIREMENTS FOR THE DEGREES OF

NUCLEAR ENGINEER
AND
MASTER OF SCIENCE IN NUCLEAR SCIENCE AND ENGINEERING
AT THE
MASSACHUSETTS INSTITUTE OF TECHNOLOGY

SEPTEMBER 2010

Signature of Author: _____

Mark A. Minton
Department of Nuclear Science and Engineering
September 10, 2010

Certified by: _____

George E. Apostolakis
Professor of Nuclear Science and Engineering and Engineering Systems
Thesis Supervisor

Certified by _____

Michael W. Golay
Professor of Nuclear Science and Engineering
Thesis Reader

Accepted by: _____

Mujid S. Kazimi
TEPCO Professor of Nuclear Engineering
Chair, Department Committee on Graduate Studies

Uncertainty and Sensitivity Analysis of a Fire-Induced Accident Scenario involving Binary Variables and Mechanistic Codes

Mark A. Minton

SUBMITTED TO THE DEPARTMENT OF NUCLEAR SCIENCE AND ENGINEERING IN PARTIAL FULFILLMENT OF THE REQUIREMENTS FOR THE DEGREES OF

NUCLEAR ENGINEER
AND
MASTER OF SCIENCE IN NUCLEAR SCIENCE AND ENGINEERING
AT THE
MASSACHUSETTS INSTITUTE OF TECHNOLOGY

SEPTEMBER 2010

ABSTRACT

In response to the transition by the United States Nuclear Regulatory Commission (NRC) to a risk-informed, performance-based fire protection rulemaking standard, Fire Probabilistic Risk Assessment (PRA) methods have been improved, particularly in the areas of advanced fire modeling and computational methods. As the methods for the quantification of fire risk are improved, the methods for the quantification of the uncertainties must also be improved. In order to gain a more meaningful insight into the methods currently in practice, it was decided that a scenario incorporating the various elements of uncertainty specific to a fire PRA would be analyzed.

The NRC has validated and verified five fire models to simulate the effects of fire growth and propagation in nuclear power plants. Although these models cover a wide range of sophistication, epistemic uncertainties resulting from the assumptions and approximations used within the model are always present. The uncertainty of a model prediction is not only dependent on the uncertainties of the model itself, but also on how the uncertainties in input parameters are propagated throughout the model. Inputs to deterministic fire models are often not precise values, but instead follow statistical distributions.

The fundamental motivation for assessing model and parameter uncertainties is to combine the results in an effort to calculate a cumulative probability of exceeding a given threshold. This threshold can be for equipment damage, time to alarm, habitability of spaces, etc.

Fire growth and propagation is not the only source of uncertainty present in a fire-induced accident scenario. Statistical models are necessary to develop estimates of fire ignition frequency and the probability that a fire will be suppressed. Human Reliability Analysis (HRA) is performed to determine the probability that operators will correctly perform manual actions even with the additional complications of a fire present.

Fire induced Main Control Room (MCR) abandonment scenarios are a significant contributor to the total Core Damage Frequency (CDF) estimate of many operating nuclear power plants. Many of the resources spent on fire PRA are devoted to quantification of the probability that a fire will force operators to abandon the MCR and take actions from a remote location. However, many current PRA practitioners feel that effect of MCR fires have been overstated.

This report details the simultaneous application of state-of-the-art model and parameter uncertainty techniques to develop a defensible distribution of the probability of a forced MCR abandonment caused by a fire within a MCR benchboard. These results are combined with the other elements of uncertainty present in a fire-induced MCR abandonment scenario to develop a CDF distribution that takes into account the interdependencies between the factors. In addition, the input factors having the strongest influence on the final results are identified so that operators, regulators, and researchers can focus their efforts to mitigate the effects of this class of fire-induced accident scenario.

Thesis Supervisor: George E. Apostolakis
Professor of Nuclear Science and Engineering and Engineering Systems

DISCLAIMER

The views expressed in this document are those of the author and do not necessarily represent the position of the Department of Defense or any of its components, including the Department of the Navy.

ACKNOWLEDGEMENTS

I would like to thank my advisor, Professor George Apostolakis, for his guidance and patience throughout the duration of this project.

I would also like to thank all of the NRC staff who have offered valuable technical advice during the performance of this work. Specifically, I would like to thank Don Helton and Nathan Siu for their helpful suggestions and insights.

Furthermore, I am especially grateful to my fellow MIT student Dustin Langewisch for his invaluable advice and assistance with some of the more computationally intensive portions of this study.

TABLE OF CONTENTS

LIST OF FIGURES

LIST OF ACRONYMS

ATHEANA	A TECHNIQUE FOR HUMAN EVENT ANALYSIS
AUX BLDG	AUXILIARY BUILDING
BE3	BENCHMARKING EXERCISE #3
CCW	COMPONENT COOLING WATER
CDF	CORE DAMAGE FREQUENCY
CFAST	CONSOLIDATED MODEL OF FIRE SMOKE AND TRANSPORT
CPSWPR	CHARGING PUMP SERVICE WATER PUMP ROOM
CV/T	CABLE VAULT/TUNNEL
EPRI	ELECTRIC POWER RESEARCH INSTITUE
ESWGR	EMERGENCY SWITCHGEAR ROOM
FDS	FIRE DYNAMICS SIMULATOR
FDTs	FIRE DYNAMICS TOOLS
FIVE-Rev1	FIRE-INDUCED VULNERABILITY EVALUATION, REVISION 1
FMAG	NUCLEAR POWER PLANT FIRE MODELING APPLICATION GUIDE
FMSNL	FACTORY MUTUAL/SANDIA NATIONAL LABORATORY
HEP	HUMAN ERROR PROBABILITY
HFE	HUMAN FAILURE EVENT
HGL	HOT GAS LAYER
HPI	HIGH PRESSURE INJECTION
HRA	HUMAN RELIABILITY ANALYSIS
HRR	HEAT RELEASE RATE
LOCA	LOSS OF COOLANT ACCIDENT
MCR	MAIN CONTROL ROOM
MIT	MASSACHUSETTS INSTITUTE OF TECHNOLOGY
NIST	NATIONAL INSTITUE OF STANDARDS AND TECHNOLOGY
NRC	UNITED STATES NUCLEAR REGULATORY COMMISSION
PDF	PROBABILITY DENSITY FUNCTION
PFS	PROBABILISTIC FIRE SIMULATOR
PORV	POWER OPERATED RELIEF VALVE
PRA	PROBABILISTIC RISK ASSESSMENT
RCC	RANK ORDER CORRELATION COEFFICIENT
RCP	REACTOR COOLANT PUMP
RES	U.S. NRC OFFICE OF NUCLEAR REGULATORY RESEARCH
RSP	REMOTE SHUTDOWN PANEL
SA	SENSITIVITY ANALYSIS
UA	UNCERTAINTY ANALYSIS
UMD	UNIVERSITY OF MARYLAND
WINBUGS	WINDOWS BAYESIAN INFERENCE USING GIBBS SAMPLING

I. EXECUTIVE SUMMARY

In response to the transition by the United States Nuclear Regulatory Commission (NRC) to a risk-informed, performance-based fire protection rulemaking standard [1], Fire Probabilistic Risk Assessment (PRA) methods have been improved [2], particularly in the areas of advanced fire modeling and computational methods [3]. As the methods for the quantification of fire risk are improved, the methods for the quantification of the uncertainties must also be improved. In order to gain a more meaningful insight into the methods currently in practice, it was decided that a scenario incorporating the various elements of uncertainty specific to a fire PRA would be analyzed.

Fire-induced Main Control Room (MCR) abandonment scenarios are a significant contributor to the total Core Damage Frequency (CDF) estimate of many operating nuclear power plants [4]. Many of the resources spent on fire PRA are devoted to quantifying the probability that a fire will force operators to abandon the MCR and take actions from a remote location. However, many current PRA practitioners [3] feel that the effects of MCR fires have been overstated. This thesis demonstrates the application of state-of-the-art techniques for analyzing the uncertainty and sensitivity of a fire-induced MCR abandonment scenario.

The NRC has validated and verified five fire models to simulate the effects of fire growth and propagation in nuclear power plants [5]. Although these models cover a wide range of sophistication, epistemic uncertainties resulting from the assumptions and approximations used within the model are always present.

For our scenario, the Consolidated Model of Fire Growth and Smoke Transport (CFAST) [6] is used to predict the evolution of environmental conditions after the

ignition of a MCR fire (Section IV). CFAST was chosen because adequate and computationally inexpensive results can be obtained for simple configurations like ours [5]. The primary simplification inherent to CFAST is the assumption that each compartment can be subdivided into two zones that are uniform in temperature and species concentration. Choosing a so-called zone model, such as CFAST, allows for much larger Monte Carlo samples to be reasonably achieved in determining model input parameter uncertainties (Section VI) and sensitivity analyses (Section X).

The upper zone in a zone model is referred to as the Hot Gas Layer (HGL). Of the MCR abandonment criteria [2], the results of this study indicate that the peak HGL temperature reached is the limiting factor in predicting forced MCR abandonment. For our scenario, the evolution of the environmental conditions predicted by CFAST reveal that the HGL layer height will descend rapidly after fire ignition, while the HGL temperature will take several additional minutes to reach a value that would force evacuation.

The general method of evaluating model uncertainty is through the comparison of model data with that of actual experiments. *A Bayesian Framework for Model Uncertainty Considerations in Fire Simulation Codes* [7], proposed by the University of Maryland (UMD), was first conducted by comparing CFAST output to experimental results contained in NUREG-1824's Benchmarking Exercise Three (BE3) [5]. Through cooperation with the United States Nuclear Regulatory Commission (NRC) and the Massachusetts Institute of Technology (MIT), the UMD method was extended to include data from the Factory Mutual/Sandia National Laboratory (FMSNL) 21 and 22 tests conducted as part of NUREG/CR-4527, *An Experimental Investigation of Internally*

Ignited Fires in Nuclear Power Plant Control Cabinets Part II: Room Effects Tests [8]. The results from the UMD method are then compared to the method presented in NUREG-1934, *Nuclear Power Plant Fire Modeling Application Guide* (FMAG) [3].

Comparison of test data from [8, 9] to model predictions shows that CFAST consistently over-predicts HGL temperature. Therefore, the most conservative method of analyzing our scenario would be to neglect model uncertainty altogether and use the values predicted by CFAST. Less conservative results can be obtained by using the method presented in the FMAG, with the UMD method yielding the least conservative results.

The uncertainty of a model prediction is not only dependent on the uncertainties of the model itself, but also on how the uncertainties in input parameters are propagated throughout the model. Inputs to deterministic fire models are often not precise values, but instead follow statistical distributions. Due to the complexity and non-linear nature of our fire model, empirical methods to estimate uncertainty propagation do not yield sufficiently refined results when multiple input parameters are allowed to vary. In order to more adequately assess the distributions of fire model output variables, Monte Carlo simulations have been coupled to our fire model, CFAST, through a tool called Probabilistic Fire Simulator (PFS) [10].

The fundamental motivation for assessing model and parameter uncertainties is to combine the results in an effort to calculate a cumulative probability of exceeding a given threshold. This threshold can be for equipment damage, time to alarm, or, for our scenario, the habitability of a MCR due to HGL temperature.

Combining current model uncertainty methods (FMAG, UMD) with parameter uncertainties (PFS) results in a reduction by a factor of approximately 20 in the mean value of the probability of forced MCR abandonment calculated in NUREG-1150.

In evaluating the combined model and parameter uncertainties present in our scenario, the goal was to develop an expression for the probability that a fire in a benchboard would force operator abandonment of the MCR if no suppression efforts were made. However, fire growth and propagation is not the only source of uncertainty present in a fire-induced accident scenario. Statistical models are necessary to develop estimates of fire ignition frequency [11] (Section III) and the probability that a fire will be suppressed [2] (Section VIII). Human Reliability Analysis (HRA) [12] (Section IX) is performed to determine the probability that operators will correctly perform manual actions even with the additional complications stemming from the presence of a fire.

The elements of uncertainty present in a fire-induced MCR abandonment scenario are combined to develop a CDF distribution that takes into account the interdependencies between the factors. The current methods used in this study show that a reduction by a factor of approximately two in the mean value of the total CDF calculated in NUREG-1150 is expected. Although this value is lower than previously assessed [4], it is still a significant contributor to total CDF and would not be eliminated in the screening process of a fire PRA.

An Uncertainty Analysis (UA) is incomplete without a discussion of which input factors have the strongest influence on the results. Sensitivity Analysis (SA) is defined by Saltelli, et al. [13] as *"[t]he study of how uncertainty in the output of a model (numerical or otherwise) can be apportioned to different sources of uncertainty in the*

model input." There are many SA methods available [14], and choosing the one that is most appropriate is important to yield meaningful results. In order to determine which input parameters have the strongest influence on the results of our fire model, PFS uses the Spearman Rank-order Correlation Coefficient (RCC) [15] to assess the sensitivity of an output value to an input parameter. RCC is independent of the distribution of the input parameters and allows the simultaneous identification of both modeling parameters and MCR properties that have the strongest influence on the peak HGL temperature achieved during our scenario [10].

The results of our case study indicate that for existing plants the one controllable factor available to an operator to mitigate the probability of a MCR abandonment scenario is the MCR ventilation rate.

For plants yet to be constructed, the effects of a MCR casualty could be substantially reduced through an improved design of the Remote Shutdown Panel (RSP) that provides the operators with the necessary cues and independent circuitry to take actions to terminate this casualty after they are forced to abandon the MCR.

The results of this study are heavily dependent on the distribution of the Heat Release Rate (HRR) of the prescribed fire. The research into HRR distributions that is currently being conducted will help to provide regulators with the necessary tools to fully assess the contribution to core damage frequency from fires initiated from within the MCR.

II. SCENARIO IDENTIFICATION

In our efforts to investigate uncertainty and sensitivity analysis methods for risk scenarios involving binary variables and mechanistic codes, we have chosen to use a fire-induced accident scenario as a case study.

To identify a fire-induced risk scenario that would yield interesting results, we considered the following sources of uncertainty specific to a fire PRA [16]:

1. Fire Ignition Frequency
2. Fire Growth and Propagation
3. Fire Suppression Probability
4. Human Error Following the Fire Event
5. Mitigating System Availability

Our analysis focused on fire-induced scenarios specific to a plant analyzed as part of NUREG-1150, *Severe Accident Risks: An Assessment for Five U.S. Nuclear Power Plants* [4], which identified five scenarios with a core damage frequency greater than 10^{-8} yr^{-1}. Four of these scenarios contribute to over 99% of the risk of core damage due to fires [17].

Three of the scenarios (fires in the Emergency Switchgear Room (ESWGR), Auxiliary Building (AUX BLDG), and Cable Vault/Tunnel (CV/T)) are similar in that a fire causes the loss of both the High Pressure Injection (HPI) and Component Cooling Water (CCW) systems. The loss of these systems leads to a reactor coolant pump (RCP) seal Loss of Coolant Accident (LOCA). The sequence of events for these scenarios is depicted in figure 2-1.

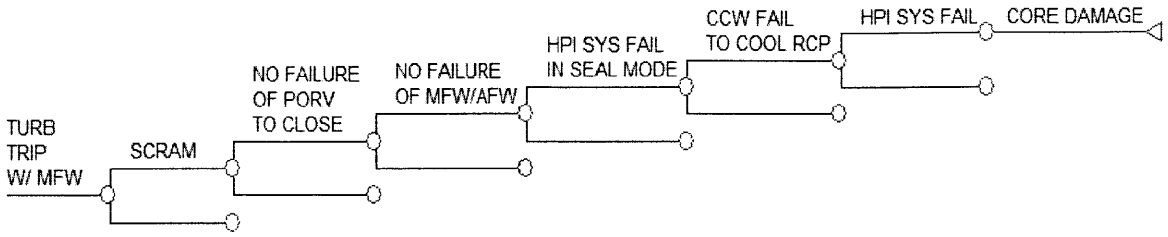

Figure 2-1: RCP Seal LOCA Sequence of Events

For the ESWGR fire, the core damage frequency equation is given in NUREG-1150 as follows:

$$CDF = \lambda_{swgr} Q(\tau_G) R_{op} [f_{a1} f_{s1} + f_{a2} f_{s2}]$$

Where:

CDF = The fire induced core damage frequency for the ESWGR.

λ_{swgr} = The frequency of ESWGR fires (of all sizes and severity).

$Q(\tau_G)$ = The percentage of fires in the data base where the fire was not manually extinguished before the COMPBRN predicted time to critical damage occurred.

R_{op} = The probability that operators will fail to cross connect the HPI system prior to a RCP seal LOCA. This does not require operators to take action in the direct vicinity of the fire.

f_{a1} = The area ratio within the ESWGR for a small fire where critical damage occurred. This is calculated by dividing the area in the ESWGR where a small fire could damage both the HPI and CCW systems by the total area of the ESWGR.

f_{s1} = The severity ratio of small fires (based on generic combustible fuel loading).

f_{a2} = The area ratio within the ESWGR for a large fire where critical damage occurred. This is calculated by dividing the area in the ESWGR where a large fire could damage both the HPI and CCW systems by the total area of the ESWGR.

f_{s2} = The severity ratio of large fires (based on generic combustible fuel loading).

For the AUX BLDG fire, the core damage frequency equation is given in NUREG-1150 as follows:

$$CDF = \lambda_{aux} f_a f_s Q(\tau_G) R_{op}$$

Where:

CDF = The fire-induced core damage frequency for the AUX BLDG.

λ_{aux} = The frequency of AUX BLDG fires.

f_a = The area ratio within the AUX BLDG where critical damage occurred.

f_s = The severity ratio for a large fire (based on generic combustible fuel loading).

$Q(\tau_G)$ = The percentage of fires within the suppression data base where the fire was not manually extinguished before the COMPBRN predicted time to critical damage occurred.

R_{op} = The probability that operators will fail to cross connect the HPI system prior to a RCP seal LOCA. This requires the operator to take action in the direct vicinity of the fire. Because of this, no recovery action was allowed until 15 minutes after the fire was extinguished.

For the CV/T fire, the core damage frequency equation is given in NUREG-1150 as follows:

$$CDF = \lambda_{csr} f_a f_s Q(\tau_G) Q_{auto} R_{op}$$

Where:

CDF = The fire-induced core damage frequency for the CV/T.

λ_{csr} = The frequency of CV/T fires.

f_a = The area ratio within the CV/T where critical damage occurred.

f_s = The severity ratio (based on generic combustible fuel loading).

$Q(\tau_G)$ = The percentage of fires in the data base where the fire was not manually extinguished before the COMPBRN predicted time to critical damage occurred.

Q_{auto} = The probability of the automatic CO_2 system not suppressing the fire before the COMPBRN predicted time to critical damage occurred.

R_{op} = The probability that operators will fail to cross connect the HPI system prior to a RCP seal LOCA. This does not require operators to take action in the direct vicinity of the fire.

The next scenario is a fire in the Charging Pump Service Water Pump Room (CPSWPR) that is caused by a general transient followed by a stuck open Power Operated Relief Valve (PORV) that leads to a small LOCA. The sequence of events for this scenario is depicted in Figure 2-2.

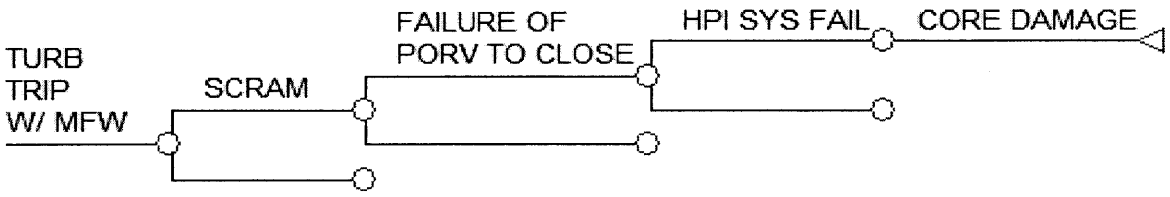

Figure 2-2: CPSWPR Sequence of Events

For the CPSWPR fire, the core damage frequency equation is as follows:

$$CDF = \lambda_{pr} Q(\tau_G) Q_{porv}$$

Where:

CDF = The fire-induced core damage frequency for the CPSWPR.

λ_{pr} = The frequency of CPSWPR fires.

$Q(\tau_G)$ = The percentage of fires in the data base where the fire was not manually extinguished before the COMPBRN predicted time to critical damage occurred.

Q_{porv} = The probability of having a stuck open PORV with failure to isolate the leak.

The final fire scenario is a fire in benchboard 1-1 that causes a spurious Power Operated Relief Valve (PORV) lift and forced Main Control Room (MCR) abandonment

followed by failure to recover the plant from the Remote Shutdown Panel (RSP). In this scenario, PORV indication is not provided at RSP and the PORV "disable" function on the RSP is not electrically independent from the MCR.

A fire-induced manual scram or turbine trip (external event) initiates the internal event tree T3-Q-D1. The sequence begins with Figure 2-3.

Where:

T3: Turbine Trip with Main Feed Water (MFW) Available.

Q: Failure of a PORV to close after transient (GO TO S2).

D1: Failure of charging pump system in High Pressure Injection (HPI) mode.

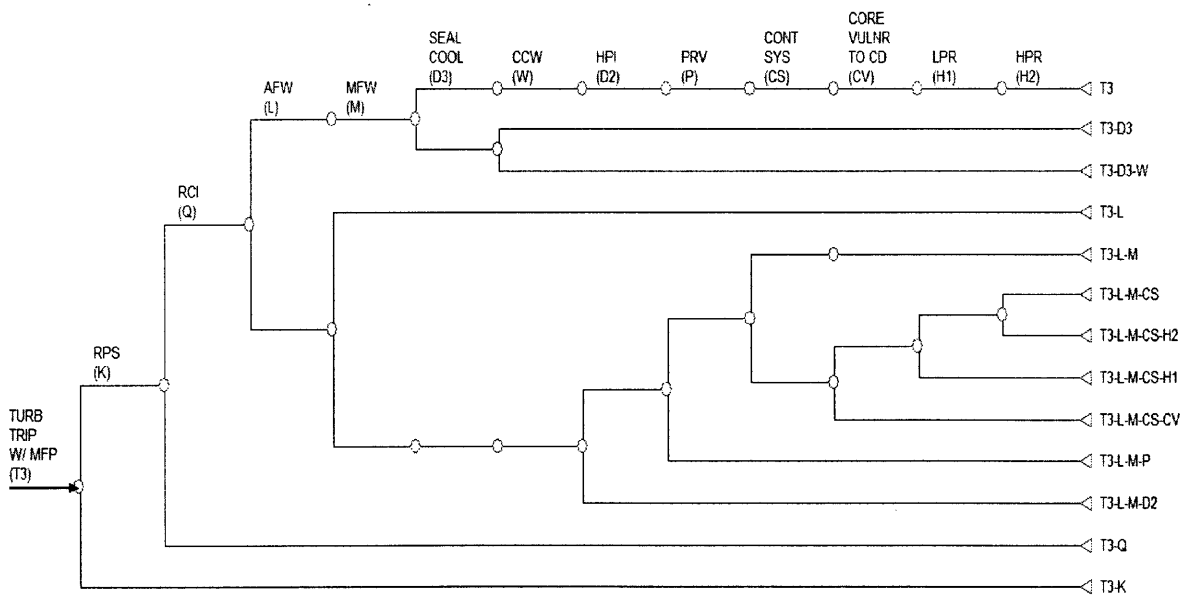

Figure 2-3: Event Tree T3- Turbine Trip with MFW Available

Once Events T3 and Q have taken place, the sequence continues on Figure 2-4, the event tree for a small LOCA. The charging system does not initiate in HPI mode because the stuck open PORV does not cause sufficient depressurization.

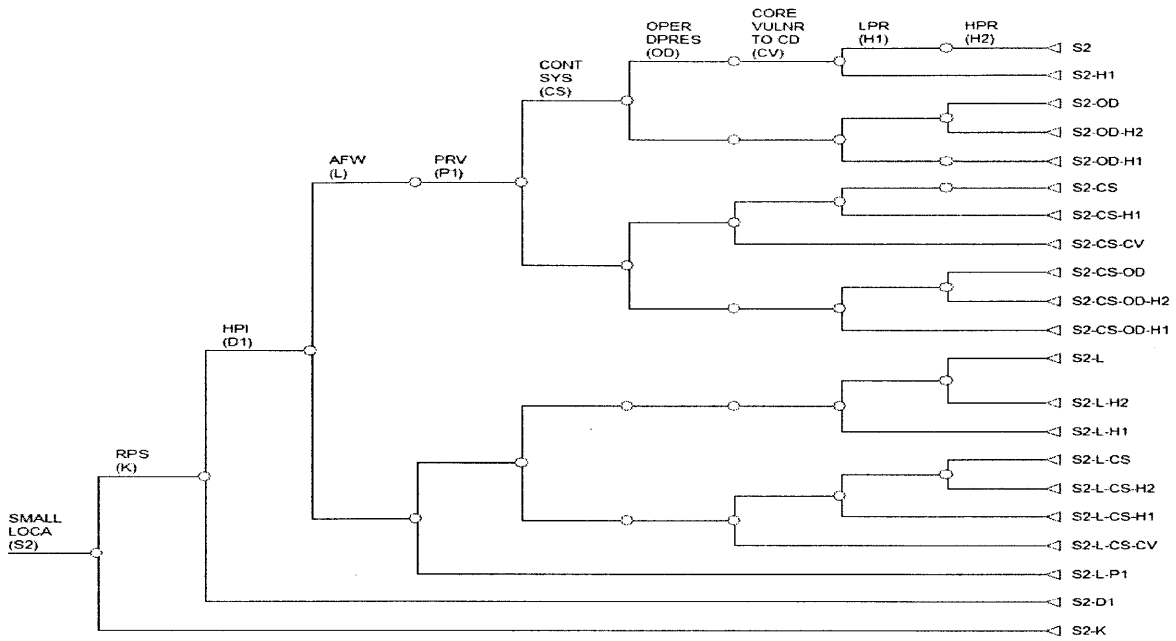

Figure 2-4: Event Tree S2-Small LOCA

Figure 2-5 shows how the fire then affects individual events in the sequence:

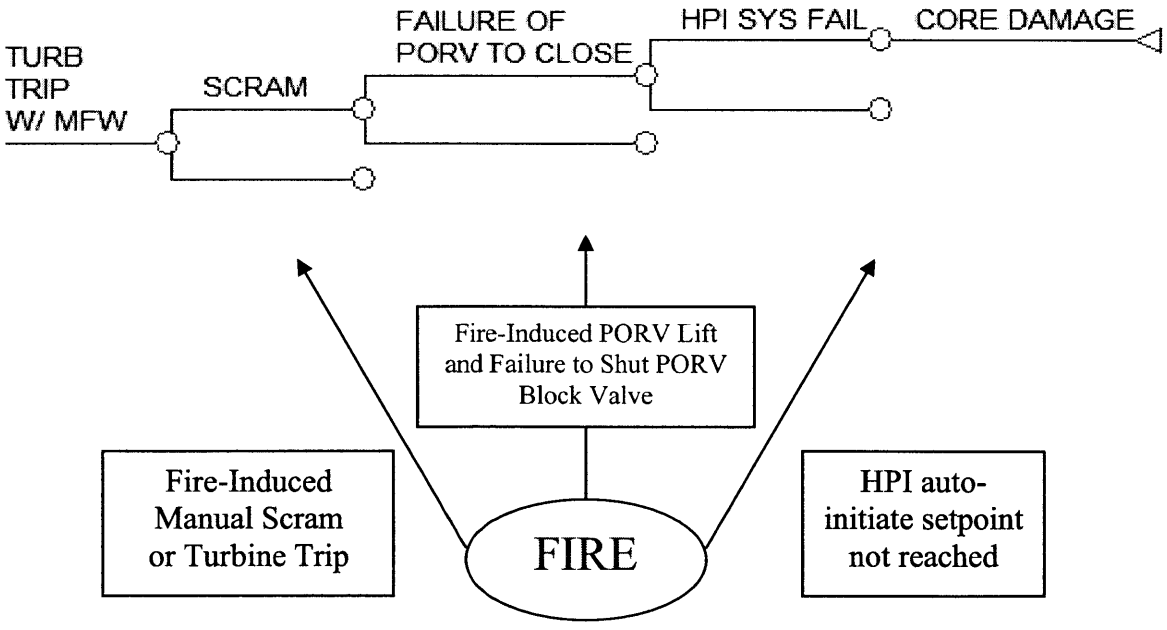

Figure 2-5: Fire Effects on Internal Sequence of Events

For the MCR fire, the core damage frequency equation given in NUREG-1150 is as follows:

$$CDF = \lambda_{cr} f_a f_r R_{op}$$

Where:

CDF = The fire-induced core damage frequency for the MCR.

λ_{cr} = The frequency of MCR fires.

f_a = The area ratio of benchboard 1-1 to total cabinet area within the MCR.

f_r = The probability that operators will not successfully extinguish the fire before forced abandonment of the MCR. According to NUREG/CR-6850, *Fire PRA Methodology for Nuclear Power Facilities: Volume 2: Detailed Methodology* [2], this requires either:

(1) Heat flux at six feet above the floor to exceed 1 kW/m^2, based on causing pain to skin, which equates to a smoke layer of 95°C. Or,

(2) The smoke layer to descend below six feet from the floor AND the smoke optical density to exceed 3.0 m^{-1}, causing the operators to be unable to see exit signs.

R_{op} = The probability that operators will unsuccessfully recover the plant from the RSP. To successfully recover the plant, the operator must shut the PORV block valve, despite not having indication on the RSP that the PORV has lifted.

Each of the scenarios under consideration would provide interesting results to the fire ignition and fire growth and propagation portions of our analysis due to the increased data and computational methods available to update the CDF distributions.

Evaluating the non-suppression of fire events is typically done through statistical methods (Section VIII) involving assessment of the time available for fire suppression before equipment damage or an operator evacuation threshold is met. These statistical models are often based on time constants derived from historical fire brigade performance data and automatic system reliability data. Because the system reliability data for automatic CO_2 systems had to be modified to account for the short time to critical damage predicted by COMPBRN, the CV/T scenario may not yield interesting results.

The CPSWPR scenario requires a signal unrelated to the fire to be sent to lift a PORV and the subsequent failure of the PORV to reclose and isolate the leak. This factor reduces the CPSWPR scenario Core Damage Frequency (CDF) contribution to less than one percent of the overall CDF due to fires. Because of this, we have eliminated the CPSWPR scenario from further consideration.

The ESWGR, CV/T and CPSWPR scenarios do not require human failure events under increased stress. Only the AUX BLDG and MCR scenarios rely on operator action in the vicinity of the fire to mitigate the sequence of events leading to core damage.

The ESWGR, AUX BLDG, and CV/T scenarios analyzed in NUREG-1150 lead to a RCP seal LOCA. Since NUREG-1150 was published, there have been improvements implemented in RCP seal technology [18, 19] that may lower the significance of re-analyzing these scenarios.

Other factors we considered are that NUREG-1824, *Verification and Validation of Selected Fire Models for Nuclear Power Plant Applications* [5], specifically covers a MCR fire scenario and has generated experimental data relating to a MCR of general

dimensions. With experimental data available, a Bayesian methodology for determining model uncertainty appears possible [7].

As we move forward, we intend to investigate methods to analyze uncertainty and sensitivity in risk scenarios induced by main control room fires.

III. FIRE IGNITION FREQUENCY

Since NUREG-1150 was published in 1990, there has been an overall downward trend in fire ignition frequency, including fires initiated in the MCR. This is expected as plants have improved fire prevention policies from lessons learned and knowledge sharing practices. Another significant factor is the decline in cigarette smoking rates nationwide.

We will now develop a distribution of fire ignition frequencies specific to our MCR abandonment scenario by applying the most updated data and methods available.

The MCR fire ignition frequency given in the NUREG-1150 analysis is a Gamma distribution characterized by a shape factor $\alpha = 1$ and scale factor $\beta = 555.56$, such that the probability density function (pdf) is given by [20]:

$$f(x \mid \alpha, \beta) = \frac{x^{\alpha-1} e^{-x/\beta}}{\beta^{\alpha} \Gamma(\alpha)}$$

Where $\Gamma(\alpha)$ is the Gamma function. The mean value of the Gamma distribution is $\alpha\beta^{-1}$. Therefore, the mean value of MCR fire ignition frequency is: $\bar{\lambda}_{cr}^{1150} = 1.8x10^{-3}\, yr^{-1}$. The resulting distribution is shown in Figure 3-1.

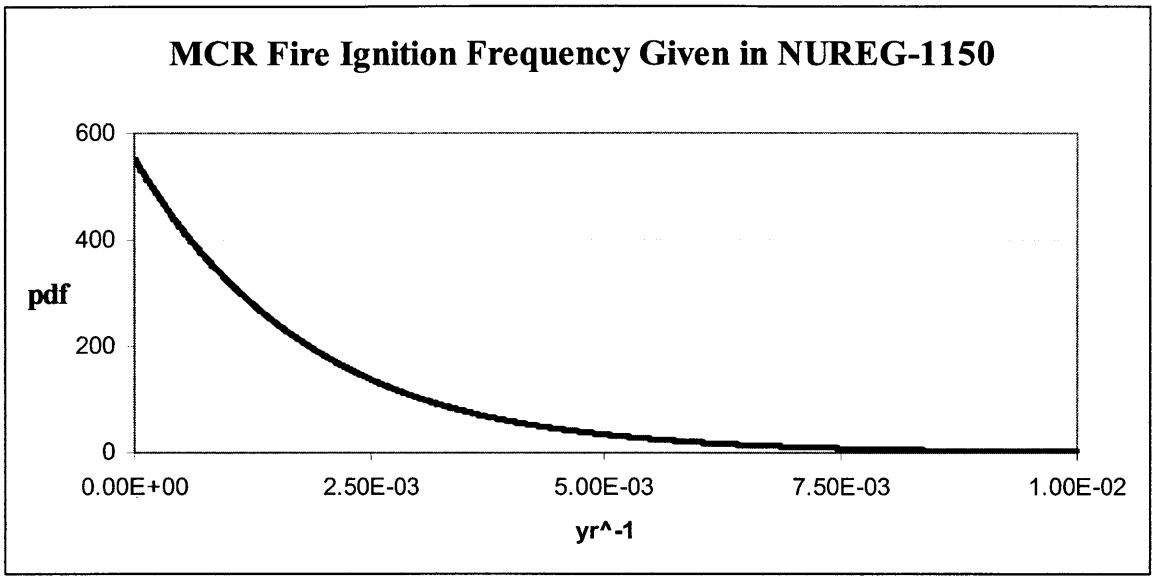

Figure 3-1: MCR Fire Ignition Frequency Given in NUREG-1150

EPRI 1016735, *Fire PRA Methods Enhancements: Additions, Clarifications, and Refinements to EPRI 101189* [11] was published in 2008 and contains the latest re-evaluation of fire ignition frequency trends and, like NUREG-1150, gives the MCR fire ignition frequency as a Gamma distribution with a shape factor of $\alpha = 1$ but differs in that a scale factor of $\beta = 1212.9$ is given. This revises the mean predicted value of MCR fire ignition frequency to: $\overline{\lambda}_{cr}^{EPRI} = 8.24x10^{-4}\, yr^{-1}$ and results in the distribution given in Figure 3-2.

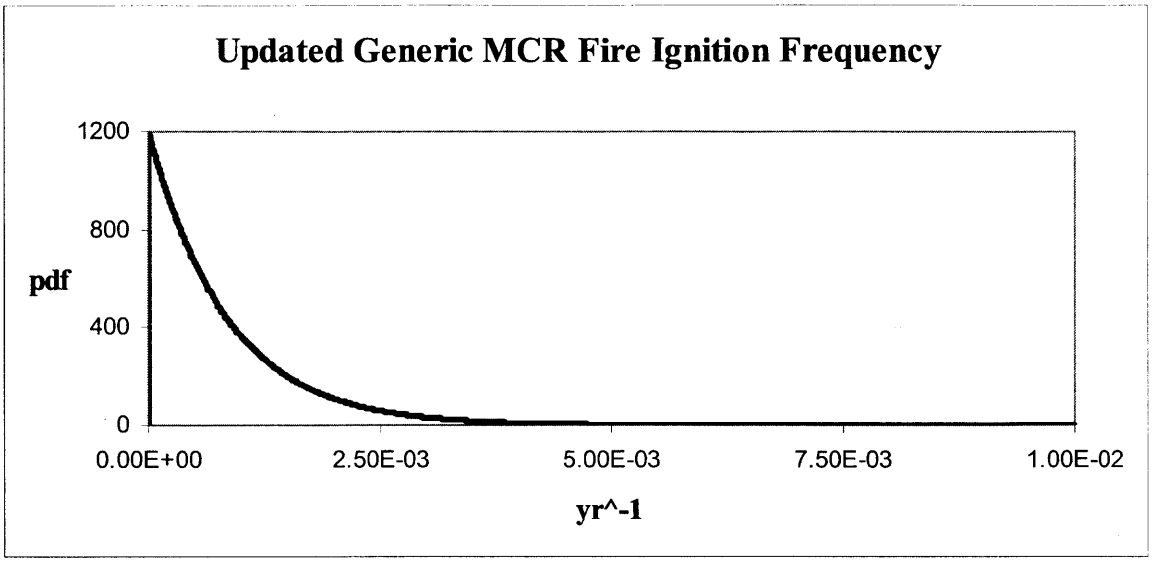

Figure 3-2: MCR Fire Ignition Frequency Given in EPRI 1016735

Using updated methods, the predicted mean MCR fire ignition frequency is a factor of 2.18 lower than previously thought.

EPRI 1016735 also contains guidance on frequency estimation parameters that can be used to update the generic fire ignition frequencies for the plant of concern. The most significant source of plant-to-plant variability appears to be the differences in event recording and reporting practices. As the practice of Fire Probabilistic Risk Assessment progresses, it will be necessary for plants to strictly adhere to standardized reporting criteria.

Simply knowing the frequency of fires that occur in the MCR is not sufficient for our analysis. For the scenario under consideration, the fire must occur in benchboard 1-1 to cause the PORV to lift. All of the event fire data to date indicate that the only source of MCR fires is electrical cabinets. In order to obtain the frequency of MCR fires that would initiate our scenario, an area ratio was developed by measuring the area of benchboard 1-1 and dividing it by the total MCR electrical cabinet area.

The area ratio of benchboard 1-1 to total cabinet area within the MCR given in the NUREG-1150 analysis is a Maximum Entropy distribution characterized by a lower bound of a = 0.028, an upper bound of b = 0.12, and a mean of μ = 0.084 such that the probability density function (pdf) is given by [21]:

$$f(\theta \mid a,b,\mu) = \frac{\beta e^{\beta\theta}}{e^{\beta b} - e^{\beta a}}$$

Where $\beta(\beta \neq 0)$ satisfies:

$$\mu = \frac{be^{\beta b} - ae^{\beta a}}{e^{\beta b} - e^{\beta a}} - \frac{1}{\beta}$$

resulting in the distribution given in Figure 3-3.

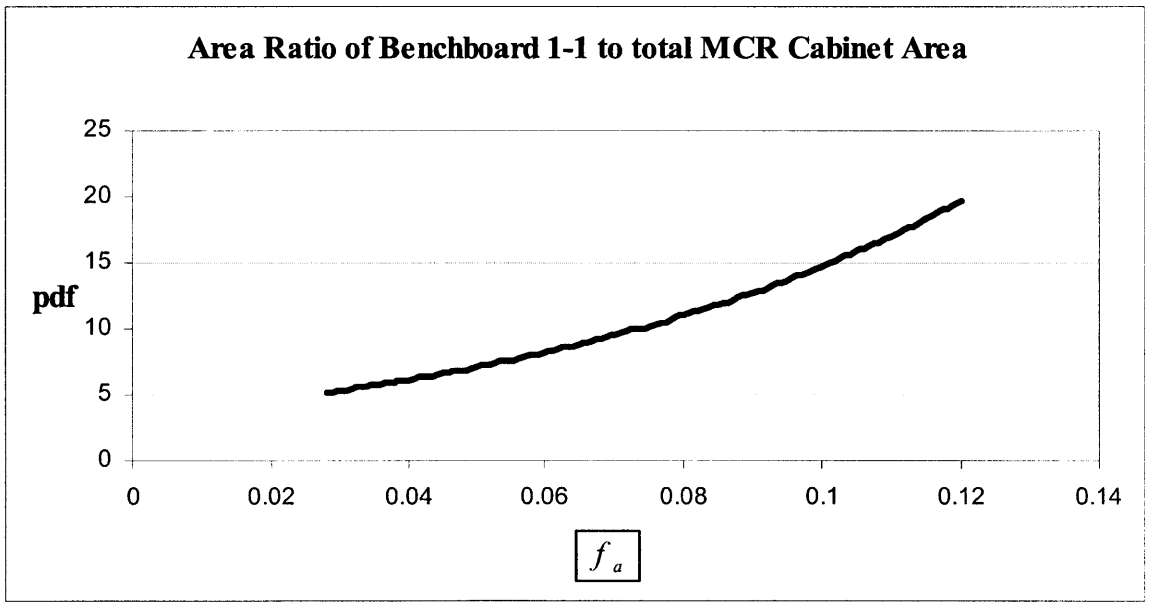

Figure 3-3: Area Ratio of Benchboard 1-1 to total MCR Cabinet Area

For this case study, it was not necessary to update the area ratio given in NUREG-1150 as the measurements obtained from the MCR are assumed to have remained the same.

In order to obtain the overall distribution of fires in benchboard 1-1, it was necessary to sample from the MCR fire ignition frequency and area ratio distributions. The resulting combined $\lambda_{cr} * f_a$ distribution is given in Figure 3-4.

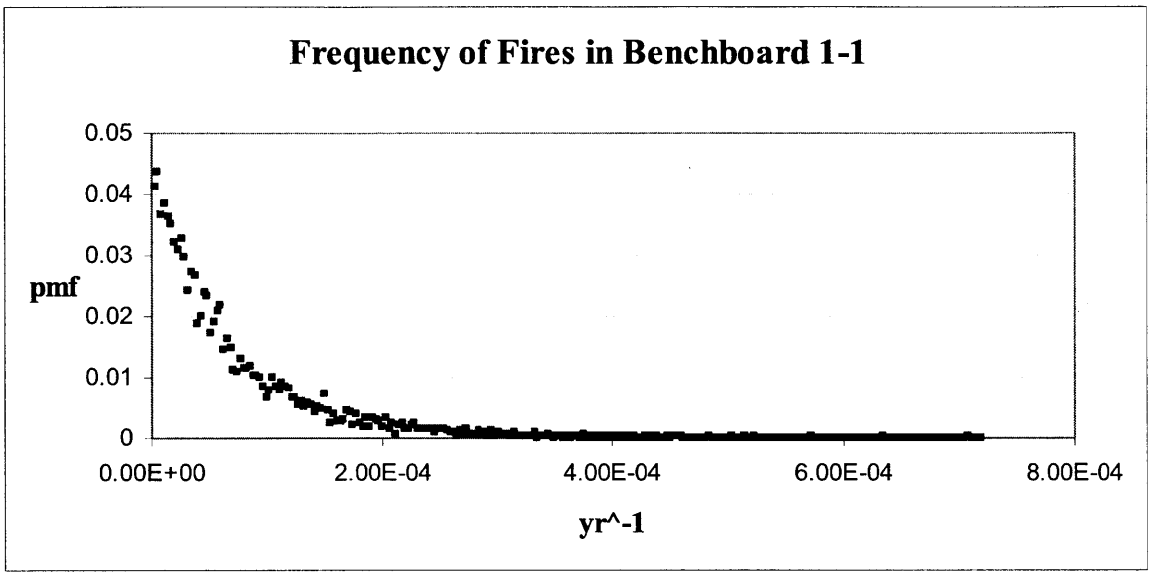

Figure 3-4: Frequency of Fires in Benchboard 1-1

The mean value of the distribution of the Frequency of Fires in Benchboard 1-1 is: $\overline{\lambda_{cr} * f_a} = 6.91x10^{-5}\, yr^{-1}$.

Now that a distribution of frequencies of initiating events has been developed, we will attempt to determine a set of environmental conditions in the MCR as a fire develops in order to determine the probability of operator abandonment given a fire in benchboard 1-1.

IV. FIRE SCENARIO MODELING

NUREG-1934, *Nuclear Power Plant Fire Modeling Application Guide (FMAG)* [3], is currently a draft for public comment that contains guidance on the use of the five fire models analyzed as a part of NUREG-1824, *Verification and Validation of Selected Fire Models for Nuclear Power Plant Applications* [5]. In modeling our MCR abandonment scenario, we will attempt to apply the guidance contained in NUREG-1934 and NUREG/CR-6850, *EPRI/NRC-RES Fire PRA Methodology for Nuclear Power Facilities: Volume 2: Detailed Methodology, TASK 11* [2]. Each of these documents contains specific guidance on the modeling of MCR fires.

Modeling Objectives

In modeling the selected scenario, our objectives are to develop an evolving set of environmental conditions in the MCR after the start of a fire in benchboard 1-1 in order to:

1. Assess the length of time the MCR remains habitable in the absence of suppression efforts by comparing environmental conditions to the MCR abandonment criteria [2]:

- Heat flux at six feet above the floor to exceed 1 kW/m^2, based on causing pain to skin, which equates to a smoke layer of 95°C.

OR

- The smoke layer to descend below six feet from the floor AND the smoke optical density to exceed 3.0 m^{-1}, causing the operators to be unable to see exit signs.

2. Provide input to detection and suppression models (Section VIII). In cases where a MCR abandonment condition is predicted to occur by the model in the absence of suppression efforts, a probability of non-suppression must be determined through assessment of the time available for suppression between fire detection and forced abandonment. In this scenario there are no installed fire suppression systems, but the MCR is continuously manned. However, because the fire takes place within a benchboard, no credit is taken for prompt detection. Redundant heat detectors are located directly above the fire and automatic detection is assumed to occur with a negligible failure probability.

3. Provide input to Human Reliability Analysis (HRA) models (Section IX). If the operators fail to suppress the fire and are forced to abandon the MCR, they will be required to take action from the Remote Shutdown Panel (RSP) under increased stress and with fewer available indications to prevent core damage.

Fire Model Selection

To identify the optimum model to analyze the scenario under consideration, the five fire models verified and validated in NUREG-1824 are considered:

(1) Fire Dynamics Tools (FDTs)

(2) Fire-Induced Vulnerability Evaluation, Revision 1 (FIVE-Rev1)

(3) Consolidated Model of Fire Growth and Smoke Transport (CFAST)

(4) MAGIC

(5) Fire Dynamics Simulator (FDS)

There are three general types of fire models. FDTs and FIVE-Rev 1 are libraries of engineering calculations, CFAST and MAGIC are zone models, and FDS is a computational fluid dynamics model.

Although FDTs and FIVE-Rev 1 provide Hot Gas Layer (HGL) temperature results, they are not suitable for this scenario because they do not provide smoke concentration or heat flux data to completely evaluate each of the MCR abandonment criteria.

FDS results have been shown to be comparable to CFAST and MAGIC, especially in simple configurations, but are computationally expensive. The single compartment MCR we will be modeling is a sufficiently simple configuration that a zone model will provide adequate results. Choosing a zone model allows for much larger Monte Carlo samples to be reasonably achieved in determining model input parameter uncertainties (Section VI) and sensitivity analyses (Section X).

In NUREG-1824, CFAST and MAGIC received identical validations for the outputs of interest in a MCR abandonment scenario. CFAST was chosen over MAGIC because it is more accessible and is well supported by the National Institute of Standards and Technology (NIST).

Fire Model Description

According to NUREG-1824, *Verification and Validation of Selected Fire Models for Nuclear Power Plant Applications, Volume 5: Consolidated Fire and Smoke Transport Model (CFAST)* [9]: "CFAST is a two-zone fire model that predicts fire-induced environmental conditions as a function of time. In order to numerically solve

differential equations, CFAST subdivides each compartment into two zones that are assumed to be uniform in temperature and species concentration."

The two publications distributed by NIST relevant to CFAST are the *CFAST Technical Reference Guide* [22], which explains the assumptions and physics of the model, and the *CFAST User's Guide* [6], which explains how to implement the model.

Fire Model Input

In 1985, Factory Mutual and Sandia National Laboratories (FMSNL) conducted a series of tests to provide data for use in validating computer fire environment simulation models, specifically MCR scenarios [8].

One of these tests (FMSNL 21) was conducted in a MCR mock-up with a fire simulated in a benchboard, similar to the scenario under evaluation. FMSNL 21 was conducted with a peak Heat Release Rate (HRR) of 470 kW, a value that is estimated to exceed the peak HRR of greater than 92% of benchboard fires. In addition, the FMSNL 21 test was conducted at a relatively low ventilation rate of one room change per hour. Sensitivity to these particular input parameters is analyzed in Section X.

Model input was chosen to mimic this test so that the output data could be compared to experimental results in the development of model uncertainty estimates (Section V). Inputs specific to the FMSNL 21 test are given in Appendices A, B, and C.

CFAST allows the user to specify the following input parameters:

(1) Ambient Conditions

(2) Compartment dimensions

(3) Construction materials and material properties

(4) Dimensions and positions of flow openings

(5) Mechanical ventilation specifications

(6) Sprinkler and detector specifications

(7) Target specifications

(8) Fire properties

NUREG-1824 states that the most important input factor is the user specified HRR. Although fire growth has been observed to follow a t^2 growth curve [23], the input to CFAST was linear. This and other assumptions and simplifications contribute to differences between predicted and observed results. Figure 4-1 shows how HRR was specified.

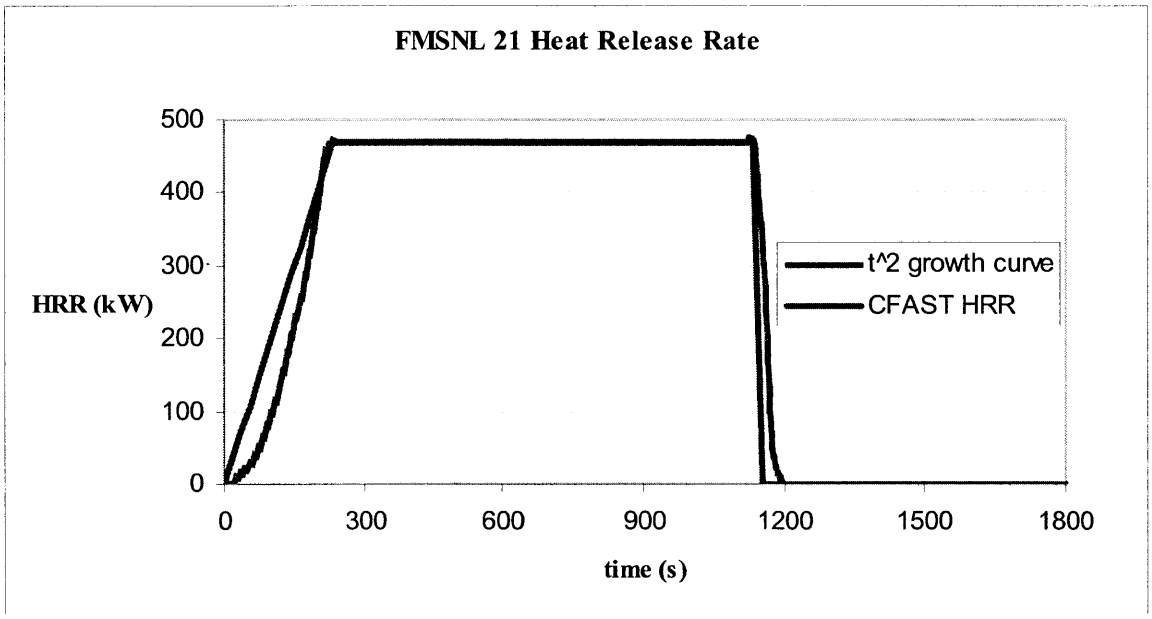

Figure 4-1: FMSNL 21 Heat Release Rate

Fire Model Generated Conditions

Each of the MCR abandonment criteria (optical density, heat flux, and HGL temperature) are conditionally dependent on the HGL descending below six feet from the floor so that the conditions actually affect the operator.

CFAST subdivides each compartment into two zones of varying volume, an upper HGL and a lower layer, with a changing interface height defined as the HGL height.

The first step in our analysis was to ensure that the MCR operators would be exposed to the conditions predicted in the HGL layer of our two zone fire model by determining the HGL height as a function of time after fire ignition.

As shown in Figure 4-2, the HGL height descends below six feet in just under five minutes.

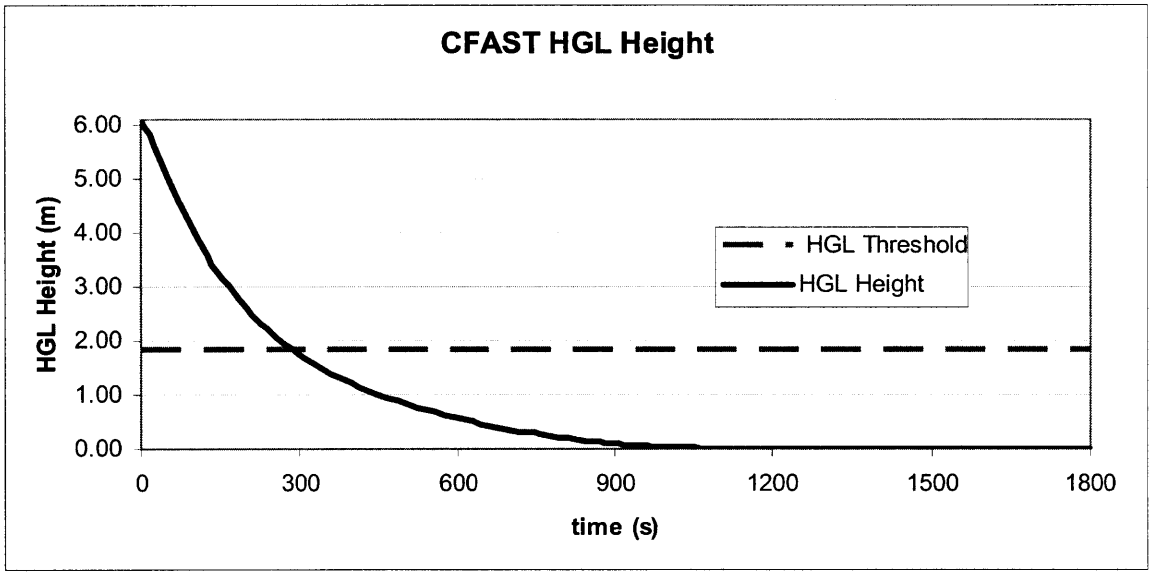

Figure 4-2: CFAST HGL Height

Once it was determined that the HGL would in fact descend to a level low enough to affect the MCR operators, each of the three MCR abandonment criteria were evaluated as a function of time.

Optical density is a measure of the transparency of smoke. It depends on the yield of different species in the soot. The higher the optical density, the lower the visibility:

$$I/I_o = e^{-\tau x}$$

Where:

I/Io = The fraction of light not scattered or absorbed.

τ = The optical density (units of length^{-1}).

x = The straight line path of length x (units of length).

In order for the optical density to force an abandonment condition, the HGL must descend below six feet from the floor (Figure 4-2) and the smoke optical density must exceed 3.0 m^{-1}. While CFAST predicts that the HGL will descend from the ceiling relatively quickly, it does not predict that the optical density threshold of 3.0 m^{-1} will be exceeded. This is shown in Figure 4-3.

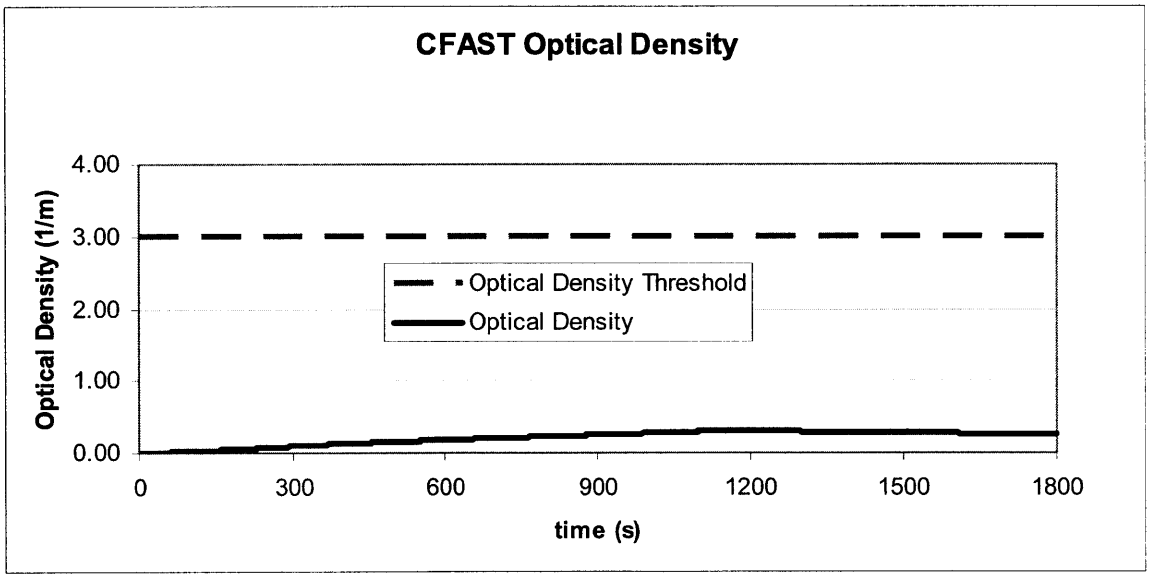

Figure 4-3: CFAST Optical Density

In addition to not predicting abandonment due to optical density, CFAST also does not predict that the heat flux will exceed the 1000 W/m^2 threshold to force the operators to abandon the MCR. This is illustrated in Figure 4-4.

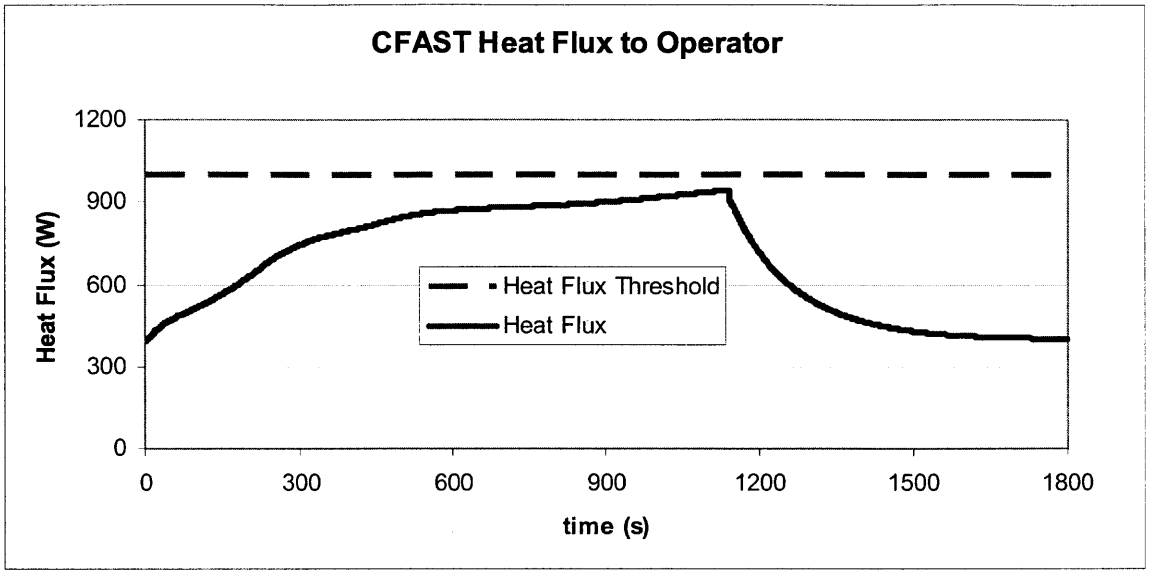

Figure 4-4: CFAST Heat Flux to Operator

CFAST predicts that the MCR will become uninhabitable in just less than 15 minutes due to the HGL temperature and height, as shown in Figure 4-5.

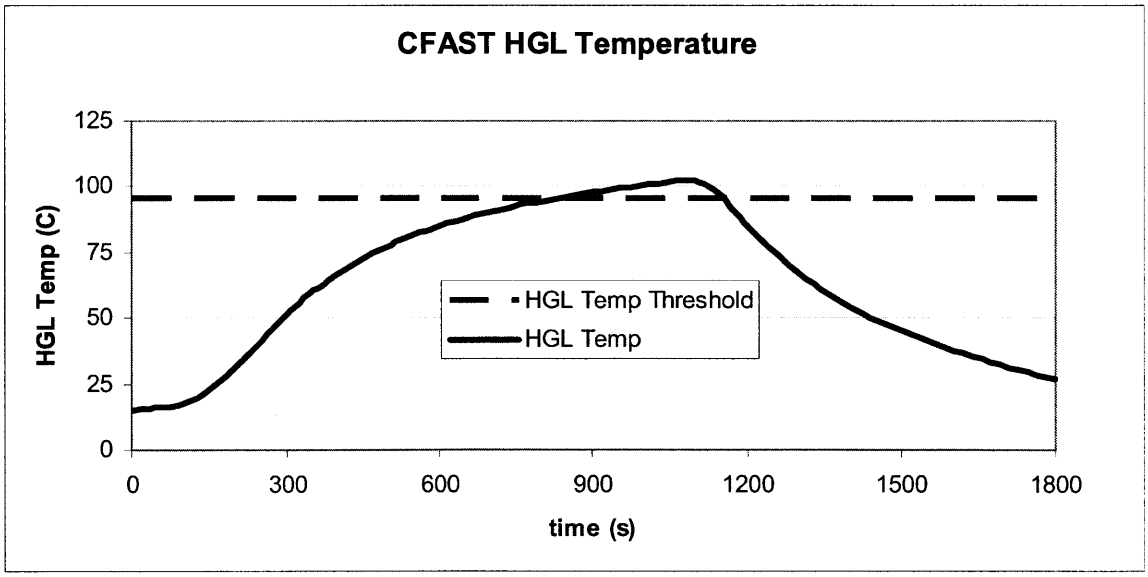

Figure 4-5: CFAST HGL Temperature

Modeling Conclusions

Even at the relatively low ventilation rate prescribed in this model, the optical density is only predicted to reach about 10% of the necessary value to force evacuation.

Although the heat flux from the smoke layer can be approximated by:

$$q_r'' = \sigma \cdot T_{sl}^4$$

Where:

q_r'' = The radiated heat flux (W/m^2).

σ = The Stefan-Boltzmann constant (5.67×10^{-8} W/m^2K^4).

T_{sl} = The temperature of the smoke layer (K).

NUREG-1824 determined that the CFAST fire model is more capable of accurately predicting HGL layer temperature and HGL height than heat flux.

HGL layer height is predicted to descend rapidly after fire ignition, while the HGL temperature is predicted to take several additional minutes to reach a value that would force evacuation.

For these reasons, I intend to focus on the HGL temperature criterion (95°C) for forced MCR abandonment.

V. MODEL UNCERTAINTY

Fire growth and propagation contains two primary sources of uncertainty. The first comes from the input, or parameter, uncertainty that occurs due to the distribution of the input parameter of interest, such as Heat Release Rate (HRR) (discussed in Section VI). The other source of uncertainty is the model uncertainty, which is the epistemic uncertainty resulting from the assumptions and approximations used within the model.

In our model, CFAST, the primary simplification is that each compartment is divided into two zones that are assumed to have uniform properties. Another simplification is made by not solving the momentum equation explicitly. However, the conservation of mass and energy equations are solved as ordinary differential equations.

For our scenario, the primary objective of assessing model uncertainty is to determine the probability of exceeding the MCR abandonment criterion of interest, HGL temperature greater than 95 °C, given a model prediction.

The general method of evaluating model uncertainty is through the comparison of model data with that of actual experiments.

A Bayesian Framework for Model Uncertainty Considerations in Fire Simulation Codes [7], proposed by the University of Maryland (UMD), was first conducted by comparing CFAST output to experimental results contained in NUREG-1824's Benchmarking Exercise Three (BE3) [9]. Through cooperation with the United States Nuclear Regulatory Commission (NRC) and the Massachusetts Institute of Technology (MIT), the UMD method was extended to include data from the FMSNL 21 and 22 tests conducted as part of NUREG/CR-4527, A*n Experimental Investigation of Internally Ignited Fires in Nuclear Power Plant Control Cabinets Part II: Room Effects Tests* [8].

The results from the UMD method using only the BE3 data (UMD BE3) are compared to the updated results determined by using the UMD method and including the FMSNL 21 and 22 test data (UMD BE3 + FMSNL 21/22). The results from the UMD method are then compared to the method presented in NUREG-1934 (FMAG) [3].

Comparison of test data from [8, 9] to model predictions show that CFAST consistently over-predicts HGL temperature. For our scenario, the discrepancy is illustrated in Figure 5-1.

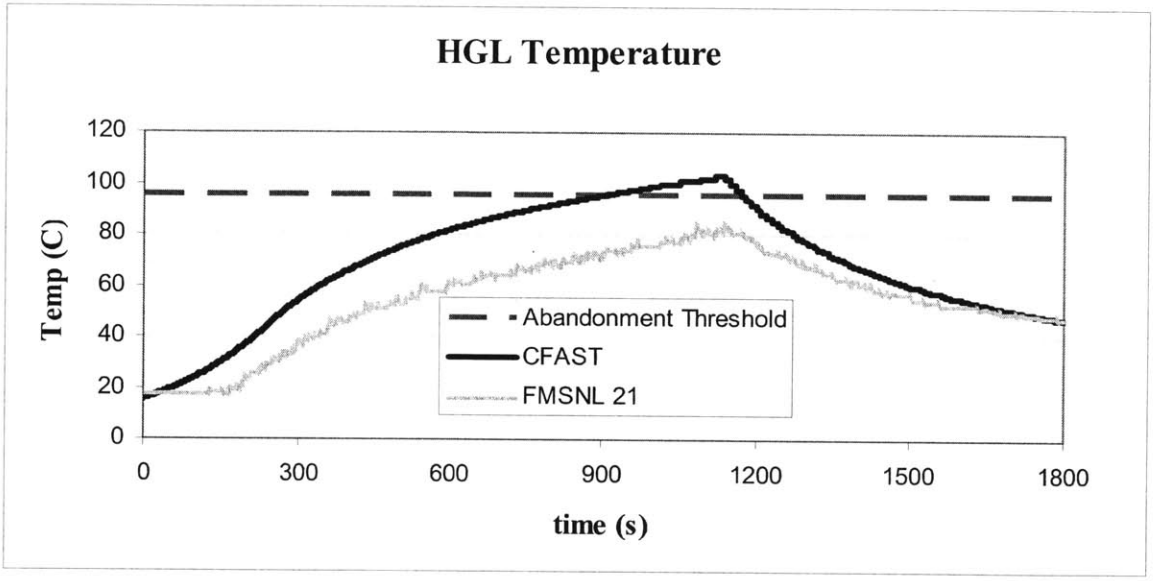

Figure 5-1: Comparison of Model Prediction to Experimentally Determined HGL Temperature

The assumptions and simplifications made by our model lead to a difference in the predicted versus experimentally determined values that is especially significant in the FMSNL 21 test case because the model predicts an abandonment condition, while the experiment does not.

Another factor that must be considered is the uncertainty present in the measurement of the FMSNL test data. The model uncertainty techniques presented here take this uncertainty, referred to as experimental uncertainty, into account.

Bayes' theorem allows a prior probability distribution to be updated to posterior probability distribution when new evidence becomes available. The new evidence, or data, is represented by a likelihood function, such that:

$$f(\theta) = \frac{L(data \mid \theta) f_o(\theta)}{\int_\theta L(data \mid \theta) f_o(\theta) d\theta}.$$

Where:

$f(\theta)$: Posterior probability distribution.

$f_o(\theta)$: Prior probability distribution.

$L(data \mid \theta)$: Likelihood of the evidence.

The UMD method [7] uses Bayesian inference to update a prior probability distribution using a likelihood function derived from the comparison of fire model output to experimental data as follows:

$$\frac{X}{X_e} = F_e$$

$$\frac{X}{X_m} = F_m$$

Substituting:

$$F_e X_e = F_m X_m$$

$$\frac{X_e}{X_m} = \frac{F_m}{F_e} = F_{em}$$

Assuming model and experimental errors are independent and log-normally distributed, the likelihood function to derive the posterior joint distribution of b_m and s_m becomes:

$$F_{em} \approx LN\left(b_m - b_e, \sqrt{s_m^2 + s_e^2}\right)$$

Where:

X: Real quantity of interest.

X_m: Model prediction.

X_e: Result of experiment.

F_m: Multiplicative error of model to real value.

F_e: Multiplicative error of experiment to the real value.

F_{em}: Multiplicative error of experiment to model prediction.

b_m: Mean, error of model to the real value.

b_e: Mean, error of experiment to the real value.

s_e: Standard deviation, error of experiment to the real value.

s_m: Standard deviation, error of model to the real value.

Once the likelihood function has been developed, the posterior joint distribution of b_m and s_m is developed as follows:

$$f(b_m, s_m \mid X_e, X_m, b_e, s_e) = \frac{f_o(b_m, s_m) * L(X_e, X_m, b_e, s_e \mid b_m, s_m)}{\int_{s_m} \int_{b_m} f_o(b_m, s_m) * L(X_e, X_m, b_e, s_e \mid b_m, s_m) db_m ds_m}$$

Where:

$$L(X_e, X_m, b_e, s_e \mid b_m, s_m) = \prod_{i=1}^{n} \frac{1}{\sqrt{2\pi}\left(\frac{X_{e,i}}{X_{m,i}}\right)\sqrt{s_m^2 + s_e^2}} \exp\left[-\frac{1}{2}x\left[\frac{\ln\left(\frac{X_{e,i}}{X_{m,i}}\right) - (b_m - b_e)}{s_m^2 + s_e^2}\right]\right]^2$$

Where:

$f_o(b_m, s_m)$: Prior joint distribution of parameters.

$f_m(b_m, s_m \mid X_{e,i}, X_{m,i}, b_e, s_e)$: Posterior joint distribution of parameters.

From this, a distribution of the real quantity of interest (X) given a model prediction (X_m) can be created using the WinBUGS (Microsoft Windows Bayesian Inference Using Gibbs Sampling) scripts included in Appendices D and E. Such that:

$$F_m \sim LN(b_m, s_m)$$

$$X = F_m X_m$$

$$X \sim LN(\ln(X_m) + b_m, s_m)$$

Figure 5-2 and Table 5-1 show the results of the UMD method, using only the BE3 data, as a comparison of a model prediction to an experimentally determined value with both experimental and model uncertainty boundaries given.

The scatter of data is assumed to result from uncertainty in both the model prediction and experimental result. Therefore, neither set of bounds should necessarily capture the entire scatter alone. Also, the experimental and model uncertainty bounds are for the real value given a model prediction, and in cases like ours in which there is a clear bias in the model prediction, the data might not fall within the bounds.

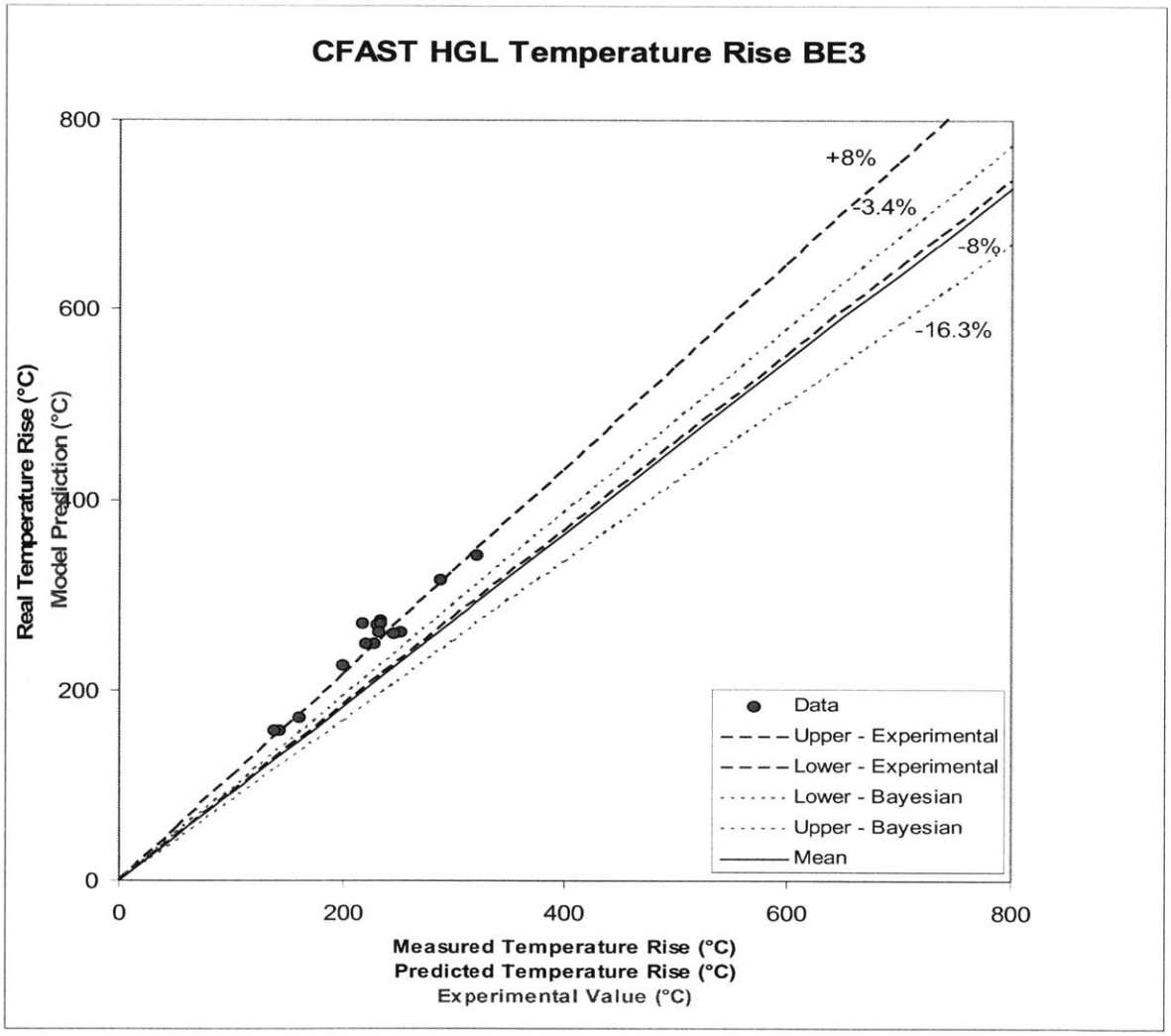

Figure 5-2: CFAST HGL Temperature Prediction vs. BE3 Experimental Data

This results in the following output data:

$F_m = 0.899$	$b_m = -0.107$	$s_m = 0.02678$

Table 5-1: UMD BE3 WinBUGS Data

which we can now use to calculate the probability of exceeding our MCR abandonment criterion of 95 °C given a model prediction (X_m):

$$\Pr(HGL > 95 \mid Xm) = 1 - \frac{1}{(2\pi)^{1/2}} \exp[-\frac{z^2}{2}]$$

Where:

$$z = \frac{\ln(95) - b_m - \ln(X_m)}{s_m}$$

Figure 5-3 illustrates how a CFAST model prediction (X_m) relates to the probability of exceeding our MCR abandonment criterion of 95 °C.

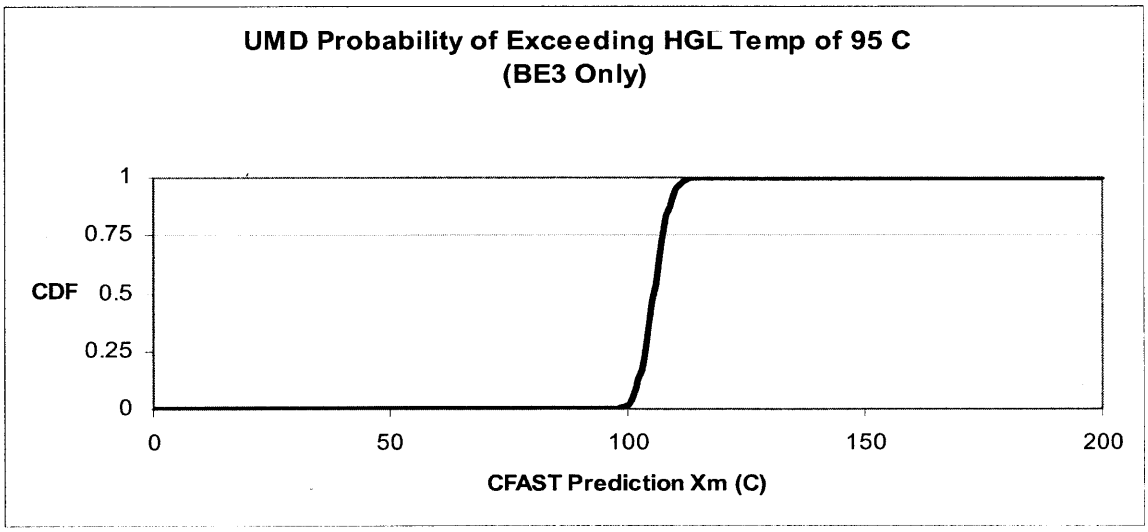

Figure 5-3: UMD BE3 Probability of Exceeding HGL Temp of 95 C

For this case study, the UMD Framework was then extended to include a comparison of CFAST output and the corresponding FMSNL tests specific to this MCR fire scenario. It is important to note that the BE3 experiments and the FMSNL test series were conducted in different geometries and with different prescribed fires. Given the

assumptions contained within the CFAST model and its known sensitivity to HRR, the additional data gained from the FMSNL test series may or may not be expected to refine the uncertainty bounds calculated using only the BE3 test data.

Figure 5-4 and Table 5-2 show the results of the UMD method, using both the BE3 and FMSNL 21/22 data, as a comparison of a model prediction to an experimentally determined value with both experimental and model uncertainty boundaries given.

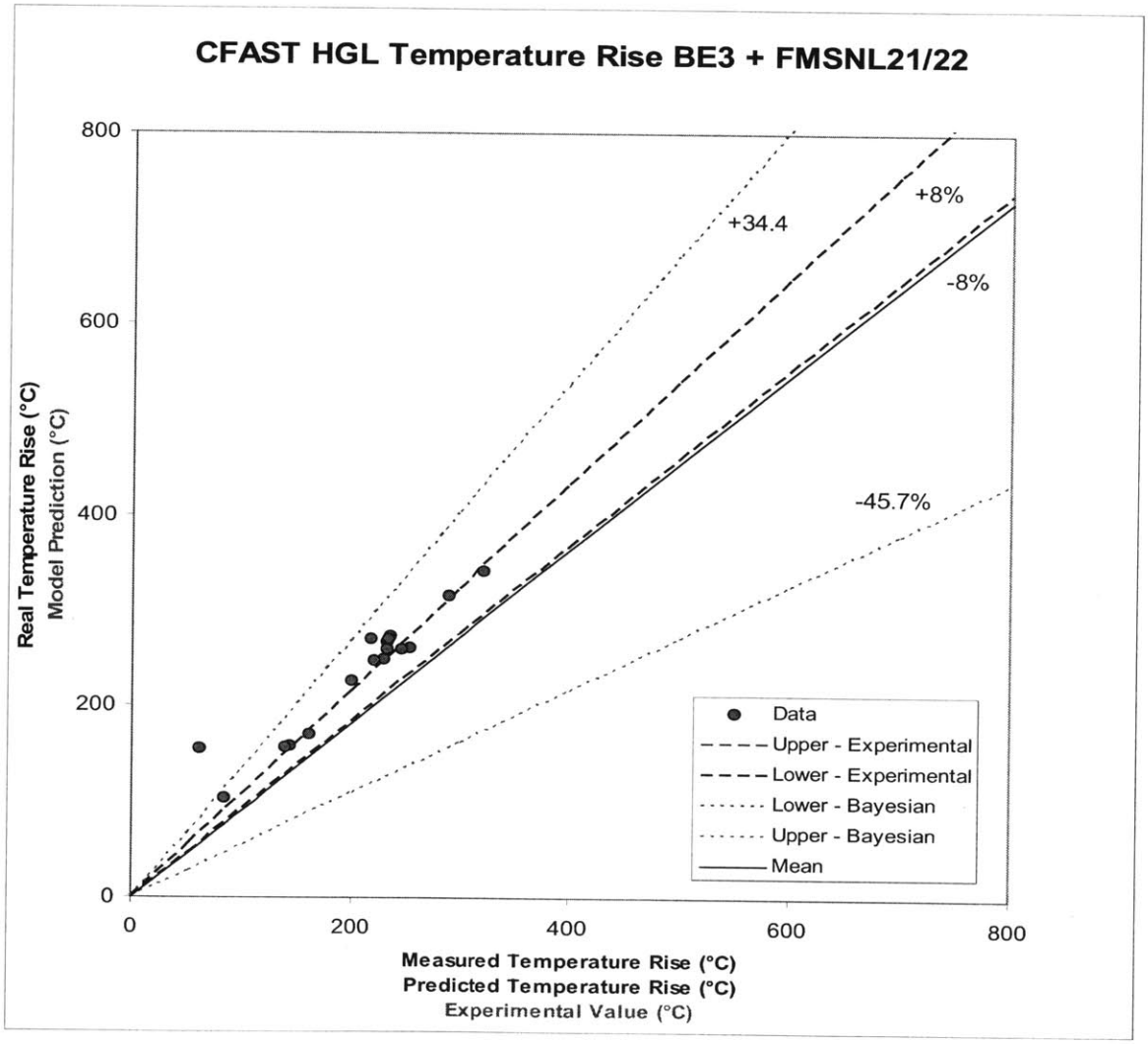

Figure 5-4: CFAST HGL Temperature Prediction vs. BE3 and FMSNL 21/22 Experimental Data

This results in the following output data:

$F_m = 0.873$	$b_m = -0.1614$	$s_m = 0.217$

Table 5-2: UMD BE3 and FMSNL WinBUGS Data

which we can now use to calculate the probability of exceeding our MCR abandonment criterion of 95 °C given a model prediction (X_m). This is illustrated in Figure 5-5.

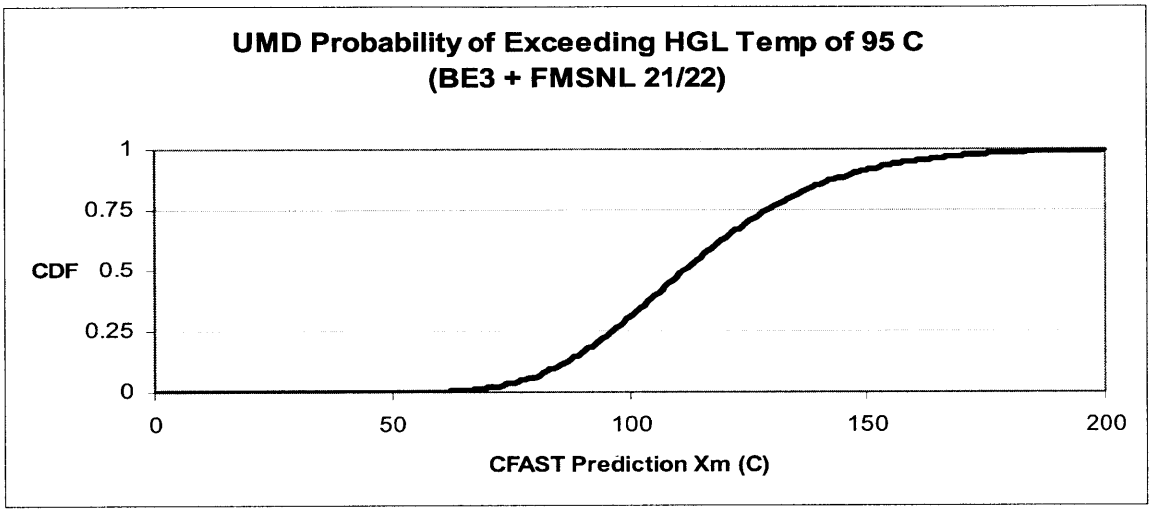

Figure 5-5: UMD BE3 Probability of Exceeding HGL Temp of 95 C

Although adding the two data points from the FMSNL 21 and 22 tests caused the uncertainty bounds predicted by the UMD method to widen, it is important not to compare these methods based on the probability of exceedance of a single model prediction only. In Section VII we will compare these methods by coupling Monte Carlo simulations to the deterministic CFAST model to determine an integrated probability of exceedance of the MCR abandonment criterion of interest.

The FMAG method uses the results of NUREG-1824 to give a bias factor and model error for each quantity of interest and fire model used while assuming model error is normally distributed such that:

$$X = N\left[\frac{X_m}{\delta}, \tilde{\sigma}_m\left(\frac{X_m}{\delta}\right)\right]$$

Where:

X: Real quantity of interest.

X_m: Model prediction.

δ: Bias factor.

$\tilde{\sigma}_m$: Relative model error.

For the CFAST model predicting HGL temperature the FMAG gives the following data:

$\delta = 1.06$	$\tilde{\sigma}_m = 0.12$

Table 5-3: FMAG Data for CFAST Predicting HGL Temperature

For the FMSNL 21 test case modeled in CFAST and predicting a peak HGL temperature of 103 °C, this results in a normal distribution with a mean of 98.02 °C and a standard deviation of 9.96 °C as shown in Figure 5-6.

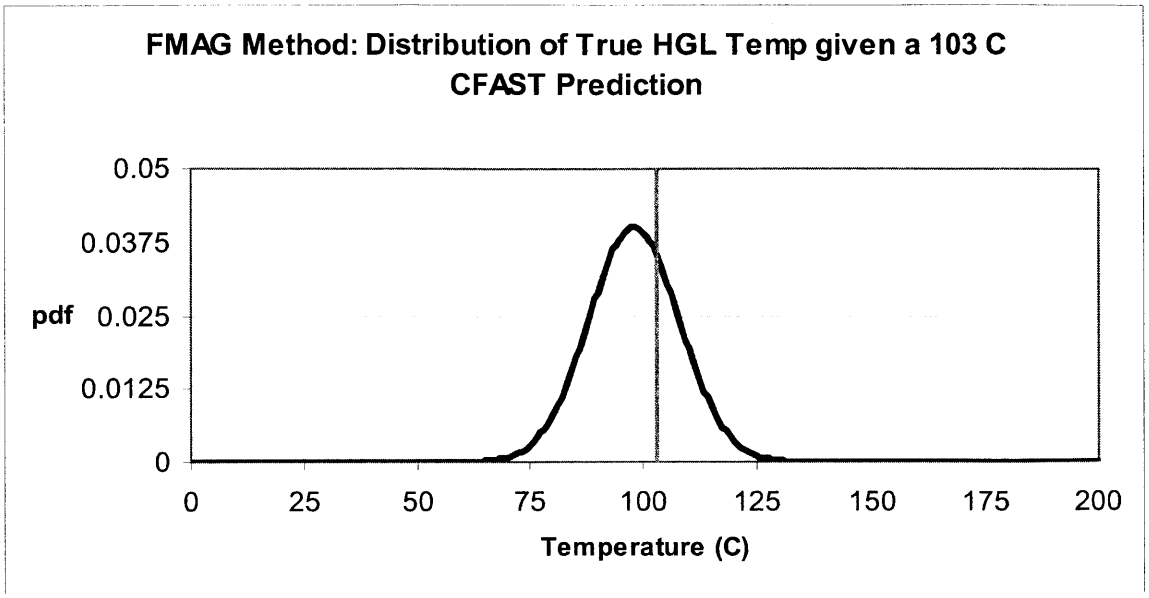

Figure 5-6: FMAG Distribution of True HGL Temp

We can now use this data to calculate the probability of exceeding our MCR abandonment criterion of 95 °C given a model prediction (X_m) and an ambient temperature of 15 °:

$$\Pr(HGL > 95 \mid Xm) = 1 - \frac{1}{(2\pi)^{1/2}} \exp[-\frac{z^2}{2}]$$

Where:

$$z = \frac{95 - \mu}{\sigma}$$

$$\mu = 15 + \frac{(Xm - 15)}{\delta}$$

$$\sigma = \tilde{\sigma}_m * \left(\frac{Xm - 15}{\delta} \right)$$

Figure 5-7 illustrates how a CFAST model prediction (X_m) relates to the probability of exceeding our MCR abandonment criterion of 95 °C.

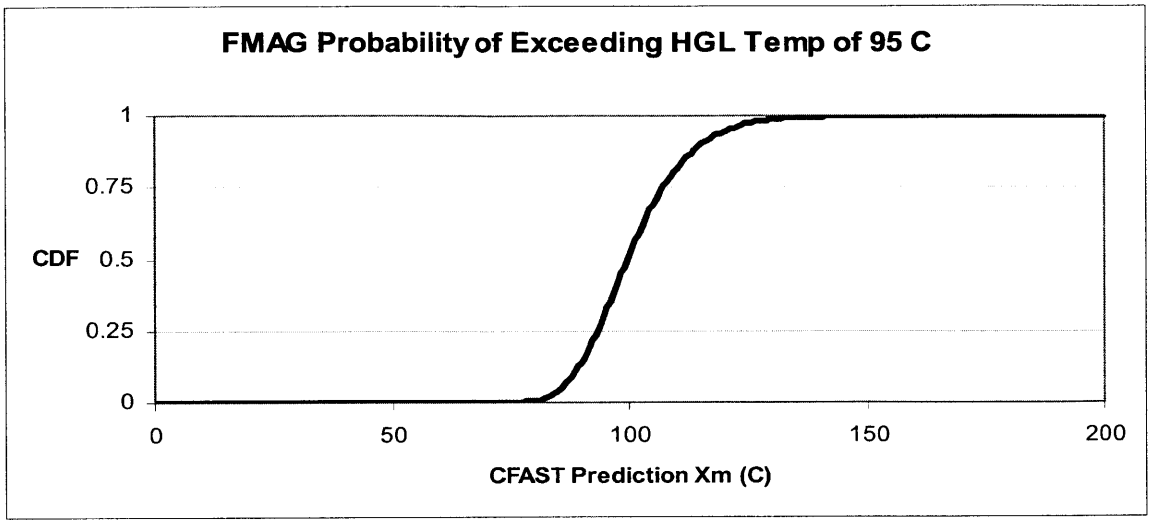

Figure 5-7: FMAG Probability of Exceeding HGL Temp of 95 C

From these results, it appears as though the method presented in the FMAG produces results that are more conservative than the UMD method. However, at this stage it would be premature to select one of the above methods of determining model uncertainty. As we move forward we will compare how each of the available methods affects the outcome of our scenario from a probabilistic standpoint by coupling Monte Carlo simulations to our deterministic fire model, CFAST, to account for the uncertainties present due to the variance in the distribution of input parameters.

VI. PARAMETER UNCERTAINTY

The uncertainty of a model prediction is not only dependent on the assumptions and simplifications of the model itself, but also on how the uncertainties in input parameters are propagated throughout the model. Inputs to deterministic fire models are often not precise values, but instead follow statistical distributions.

In simple cases, when the effect on a single output quantity due to changing just one input parameter is desired, empirical correlations may be appropriate. NUREG-1934 [3] offers very useful guidance on the use of model-independent empirical correlations that provide one-to-one mapping of the effect on a specific output quantity given a change in a single input parameter. For our scenario, where HRR is the most significant input parameter [9] and the HGL temperature is the output quantity we desire to calculate, the McCaffrey, Quintiere, and Harkleroad (MQH) correlation [24] is given:

$$T_{HGL} - T_{HGL_o} = C * (HRR)^{2/3}$$

Where:

T_{HGL} = Hot Gas Layer Temperature.

T_{HGL_o} = Initial Hot Gas Layer Temperature.

C = Constant.

HRR = Heat Release Rate.

The value of the constant is irrelevant, as the relationship we are seeking is developed by differentiating the MQH correlation with respect to HRR:

$$\frac{\Delta T_{HGL}}{T_{HGL} - T_{HGL_o}} = \frac{2}{3} * \frac{\Delta HRR}{HRR}$$

Where:

$\frac{\Delta T_{HGL}}{T_{HGL} - T_{HGL_o}}$ = Relative Change in HGL Temperature Output.

$\frac{\Delta HRR}{HRR}$ = Relative Change in HRR Parameter Input.

From the MQH correlation, it is expected that a 15% increase in HRR would lead to a 10% increase in HGL Temperature. Figure 6-1 shows a comparison the FMSNL 21 CFAST simulation with HRR increased by 15% compared to the value predicted by the MQH correlation.

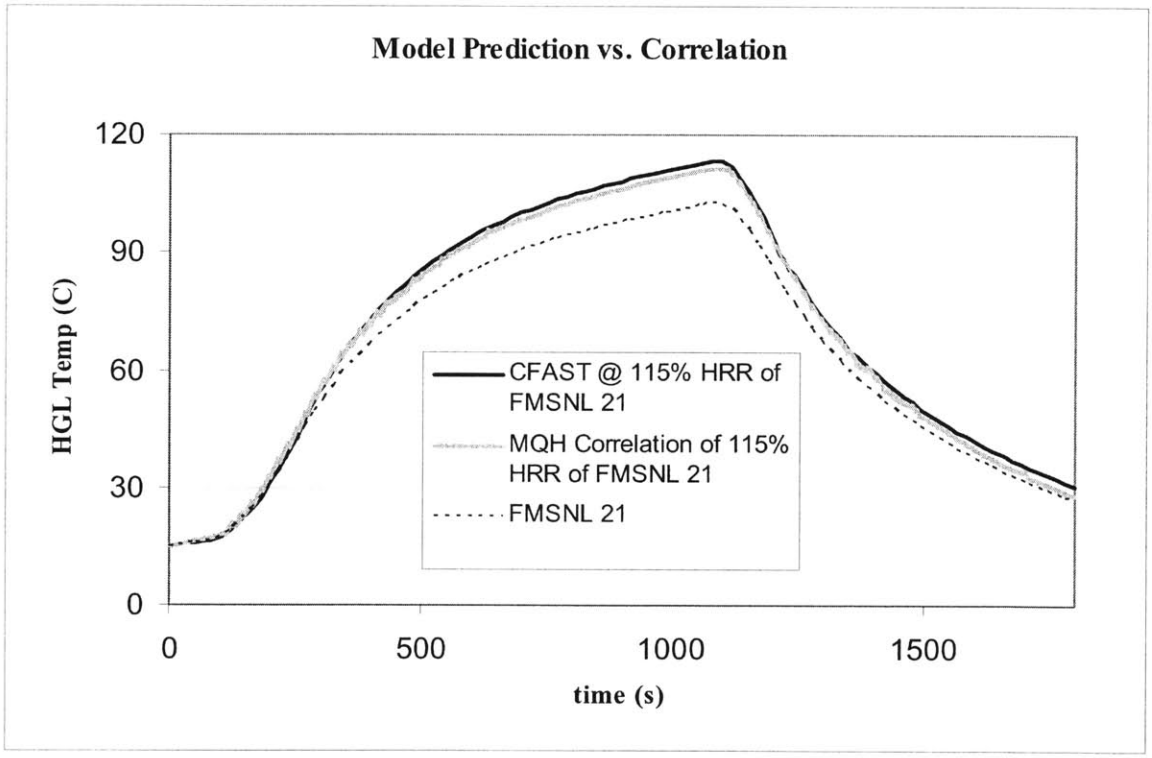

Figure 6-1: Comparison of CFAST Output to MQH Prediction

From Figure 6-1 it is apparent that the MQH correlation is useful when only one input parameter is subject to variability.

Due to the complexity and non-linear nature of our fire model, empirical methods to estimate uncertainty propagation do not yield sufficiently refined results when multiple input parameters are allowed to vary. In order to more adequately assess the distributions of fire model output variables, Monte Carlo simulations have been coupled to our fire model, CFAST, through a tool called Probabilistic Fire Simulator (PFS) [10]. PFS also gives the sensitivity of the output variables to the input variables in terms of rank order correlation coefficients (Section X).

We are primarily concerned with determining the probability that the peak HGL temperature reached in our MCR fire scenario, as predicted by CFAST, will exceed the 95 °C threshold for MCR abandonment in the absence of suppression efforts. A secondary goal of interest is to assess the time available for suppression efforts by comparing the detector activation time with the time of forced abandonment. PFS provides the necessary time series data for this evaluation.

Once the probability that an abandonment condition in the absence of suppression efforts has been determined, the parameter uncertainty and model uncertainty results will be combined (Section VII) to determine an integrated probability of exceeding the specified abandonment criterion in the absence of suppression efforts.

Suppression efforts will then be factored in through an assessment of the evolution of environmental conditions in the MCR with time compared to detector activation data (Section VIII). From this, an estimate of operator abandonment of the MCR, given a fire in benchboard 1-1, will be obtained.

Prior to fully implementing PFS, it was necessary to first use the spreadsheet environment to duplicate the modeling results obtained in Section IV in order to

demonstrate proper operation. The PFS input specifically designed to mimic the FMSNL 21 test is given in Appendix F.

Once fully implemented, PFS couples Monte Carlo simulations with CFAST in a spreadsheet environment that allows the user to vary input parameters with individually specified distributions.

From NUREG-1824 [9] it is known that CFAST is especially sensitive to variations in HRR. In order to adequately model the HRR distribution during a fire, both the initial growth period and the fully developed state (HRR_{max}) must be considered.

Fire growth has been observed to follow a t^2 growth curve [23] up to a fully developed state where the HRR becomes equal to HRR_{max}, such that:

$$HRR(t) = \min\left\{ HRR_{\max}, 1000 * \left(\frac{t}{t_g} \right)^2 \right\}$$

Where:

HRR(t) = Heat Release Rate as a function of time.

HRR_{max} = Maximum HRR attained during the fire scenario.

t = Time after fire ignition.

t_g = HRR growth time.

For our scenario, t_g is treated as a normally distributed random variable with a mean of 320 seconds and a standard deviation of 100 seconds, consistent with [10]. Figure 6-2 shows how variations in t_g affect the HRR distribution of the FMSNL 21 case.

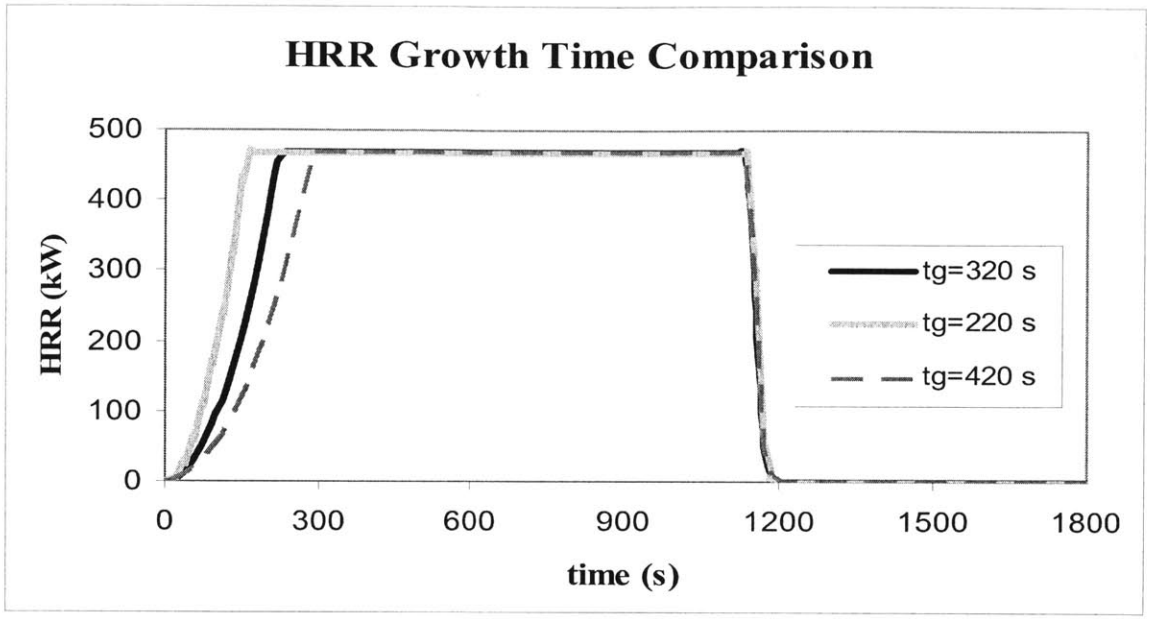

Figure 6-2: Comparison of HRR Distributions Given Variations in Growth Time

The maximum value that HRR reaches in each simulation (HRR_{max}) used in this case study is given in Appendix G of NUREG-6850 [2] as a Gamma distribution characterized by a shape factor $\alpha = 0.7$ and scale factor $\beta = 216$, such that the probability density function (pdf) is given by [20]:

$$f(x \mid \alpha, \beta) = \frac{x^{\alpha-1} e^{-x/\beta}}{\beta^{\alpha} \Gamma(\alpha)}$$

Where $\Gamma(\alpha)$ is the Gamma function. The mean value of the distribution is $\alpha*\beta$. The mean value of HRR_{max} given in Appendix G of NUREG-6850 is:

$\overline{HRR}^{6850} = 151.2kW$ resulting in the distribution given in Figure 6-3.

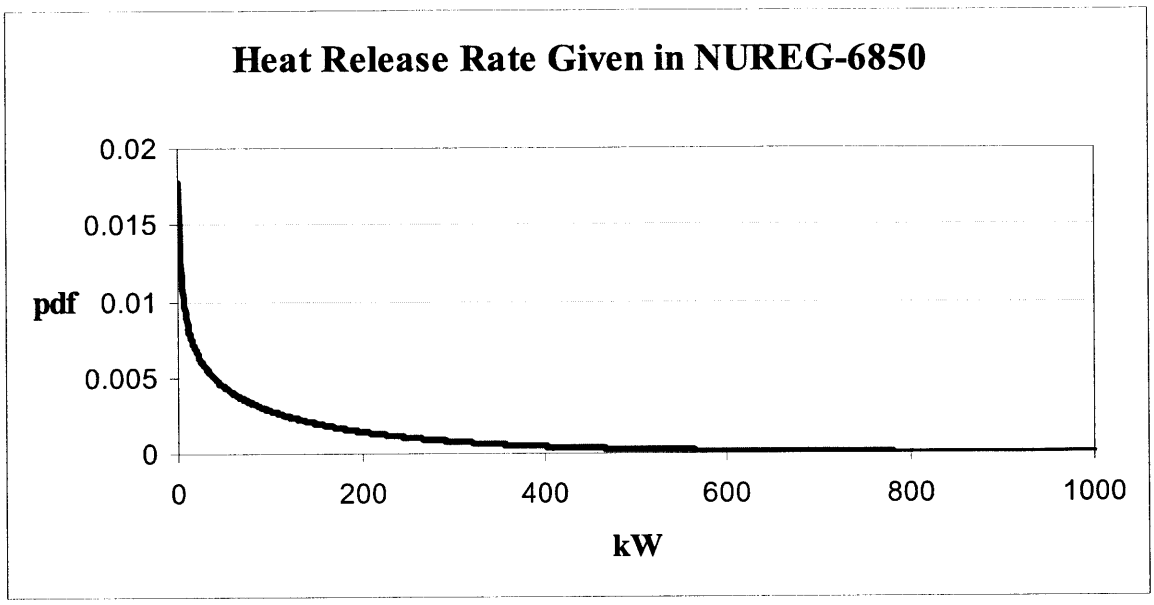

Figure 6-3: NUREG-6850 Appendix G HRR for Cabinets with Qualified Cable

Once the HRR distribution input to PFS was specified, it was also determined that we would vary the environmental and thermodynamic properties that could have an outcome on the fire scenario analysis. Table 6-1 lists the random variables used in our scenario with their associated distributions specified as input to PFS.

VARIABLE	DISTRIBUTION			UNITS
Heat Release Rate	Gamma	alpha = 0.7	beta = 216	kW
HRR Growth Time	Normal	mean = 320	s.d. = 100	M
Ventilation Rate	Uniform	min = 0.38	max = 1.90	m^3/s
Lower Oxygen Limit	Uniform	min = 9.00	max = 11.00	%
Relative Humidity	Uniform	min = 45.00	max = 55.00	%
Radiative Fraction	Uniform	min = 0.315	max = 0.3850	
Heat of Combustion	Uniform	min = 4.05e4	max = 4.95e4	(kJ/kg)
Wall Conductivity	Uniform	min = 0.108	max = 0.132	W/m*K
Wall Specific Heat	Uniform	min = 1250	max = 1375	J/kg*K
Wall Density	Uniform	min = 720	max = 2200	kg/m^3
Wall Thickness	Uniform	min = 0.0225	max = 0.275	M
Wall Emissivity	Uniform	min = 0.855	max = 1.045	

Table 6-4: Random Variables Used

For each simulation, a CFAST input file is created from both the fixed data and the samples drawn from random variables within the above constraints. CFAST is then run to generate and save time series data of the user's choice for each simulation. For our scenario it was necessary to generate detector activation time data, HGL temperature time series data, and a record of the peak HGL temperature achieved in each simulation.

Convergence criteria were set so that the sample size (n) would be sufficiently large to obtain meaningful results while remaining computationally inexpensive. For our scenario, we were interested in determining the probability that that a given fire would have a predicted peak HGL temperature in excess of 95 °C within the following constraints:

$$\left| \frac{\Pr(T > 95C)^{n} - \Pr(T > 95C)^{n+1000}}{\Pr(T > 95C)^{n+1000}} \right| \leq 0.01$$

Reaching our convergence criteria required 10,000 samples, as illustrated in Figure 6-4.

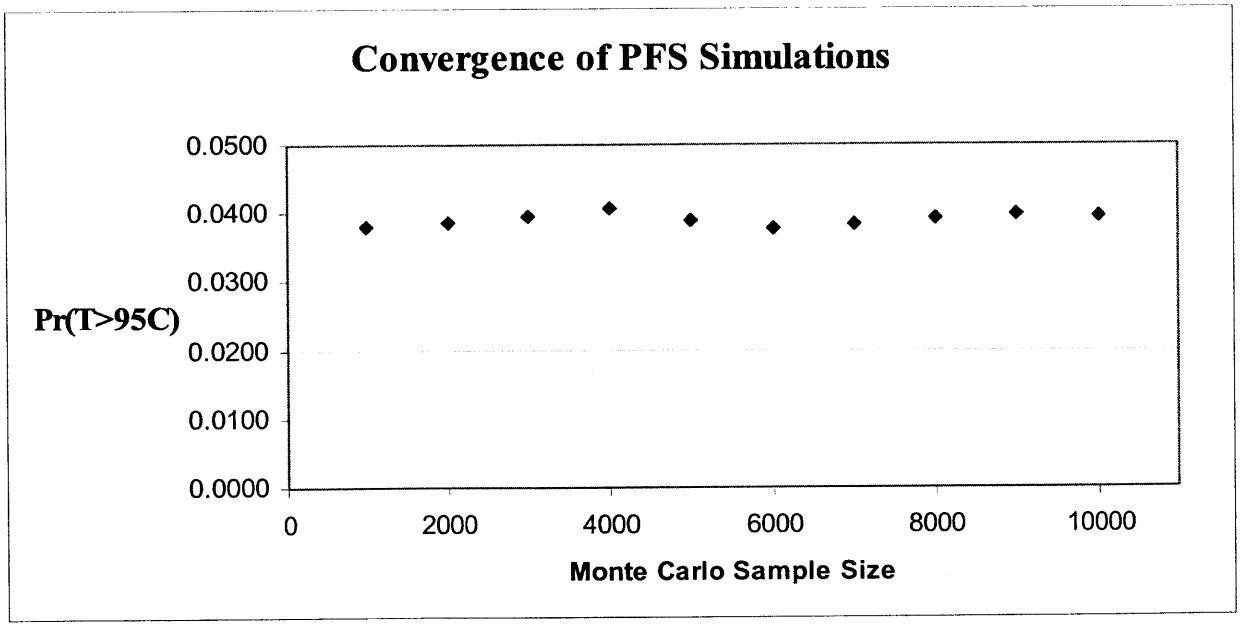

Figure 6-4: Convergence of Probabilistic Fire Simulator Results

The distribution of peak HGL temperature predictions by PFS is shown in Figure 6-5 as a probability mass function (pmf).

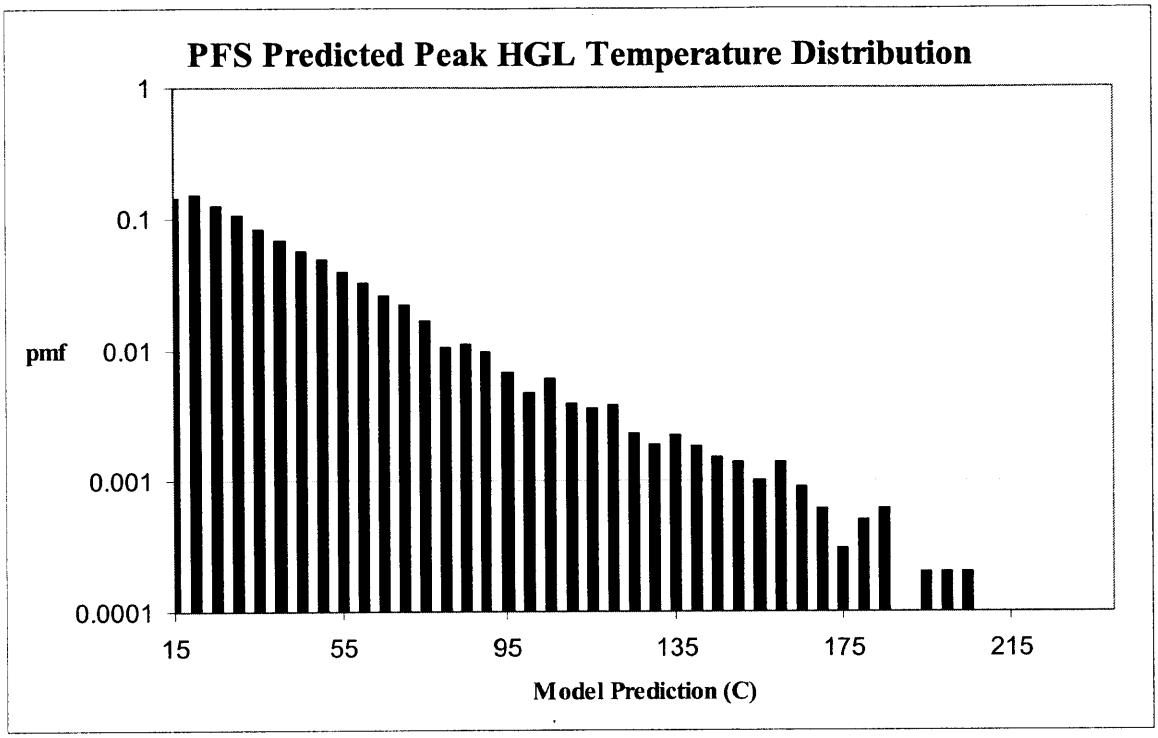

Figure 6-5: Peak Predicted HGL Temperature Distribution Prediction

Once the distribution of peak HGL temperatures is known, the probability that an abandonment condition will be reached can be derived from the cumulative distribution function (CDF) of peak predicted HGL temperature given in Figure 6-6, such that:

$$CDF = \int_0^{\infty} pmf(T_{HGL})dT_{HGL}$$

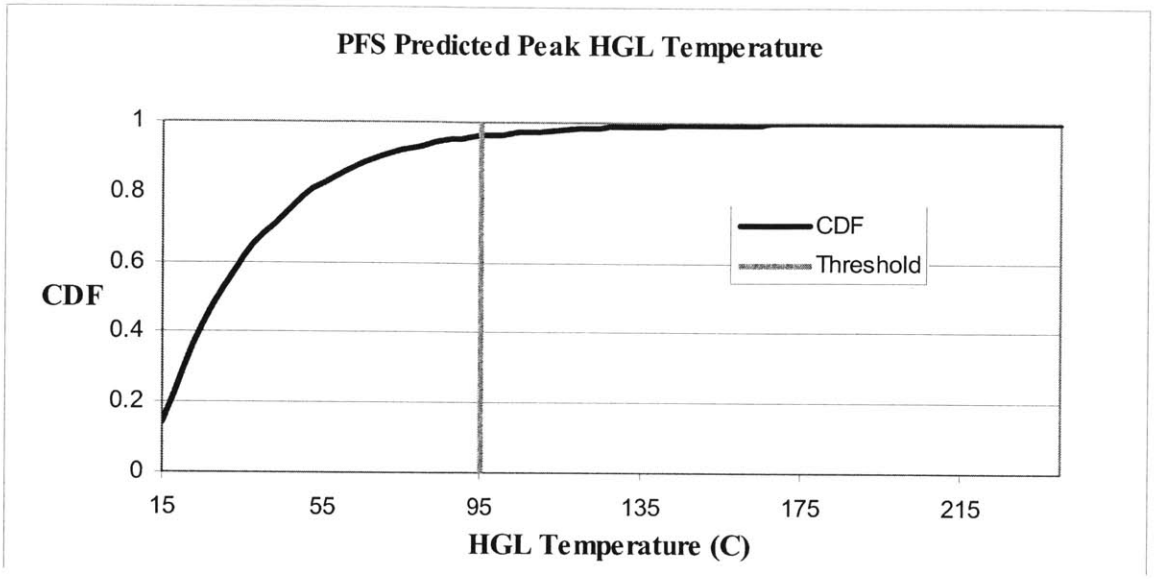

Figure 6-6: Cumulative Distribution Function of Peak Predicted HGL Temperature

The probability of reaching an abandonment condition is then calculated as:

$$\Pr(T > 95C) = 1 - \int_{0}^{95} pmf(T_{HGL})dT_{HGL}$$

This results in:

$$\Pr(T > 95C) = 0.0395$$

This quantity represents a conservative estimate of the probability of operator abandonment of the MCR given a fire in benchboard 1-1. In Section V it was determined that our CFAST fire model consistently over-predicted peak HGL temperature. In order to refine this estimate it will be necessary to combine model and parameter uncertainties (Section VII) and account for suppression efforts (Section VIII) taken by the operators in the MCR.

VII. COMBINED MODEL AND PARAMETER UNCERTAINTY

Now that we have developed separate techniques for assessing model and parameter uncertainties, our next task is to combine the methods in an effort to calculate a cumulative probability of exceeding our MCR abandonment threshold given a fire in benchboard 1-1 and assuming no suppression efforts are made.

If the only input parameter that we intended to vary was HRR, and if the HRR distribution was known and normally distributed, we could combine the NUREG-1934 (FMAG) model uncertainty (also normally distributed) and parameter uncertainty via quadrature, such that [3]:

$$\tilde{\sigma} = \sqrt{\tilde{\sigma}_M^2 + p^2 \tilde{\sigma}_I^2}$$

Where:

$\tilde{\sigma}$ = The standard deviation of the combined error.

$\tilde{\sigma}_M$ = The standard deviation of the model error.

p = A sensitivity factor (2/3 for HGL temperature).

$\tilde{\sigma}_I$ = The standard deviation of the input (parameter) error.

However, the FMAG method is not applicable to our case study because the parameter that we are most sensitive to, HRR, is not normally distributed nor is it the only input parameter to be varied.

In Section V we presented model uncertainty techniques that provide a probability of exceeding a threshold given a single model prediction, X_m. We will now extend this framework to handle a distribution of model predictions (Figure 6-5) that is created when input parameters are allowed to vary as specified in Section VI (Table 6-1).

Each of the model uncertainty techniques covered in Section V suggest that the true value that peak HGL temperature reaches is less than that predicted by CFAST (being run by PFS). Figure 7-1 shows a comparison of our model uncertainty techniques by the mean value of the peak HGL temperature predicted in each model simulation.

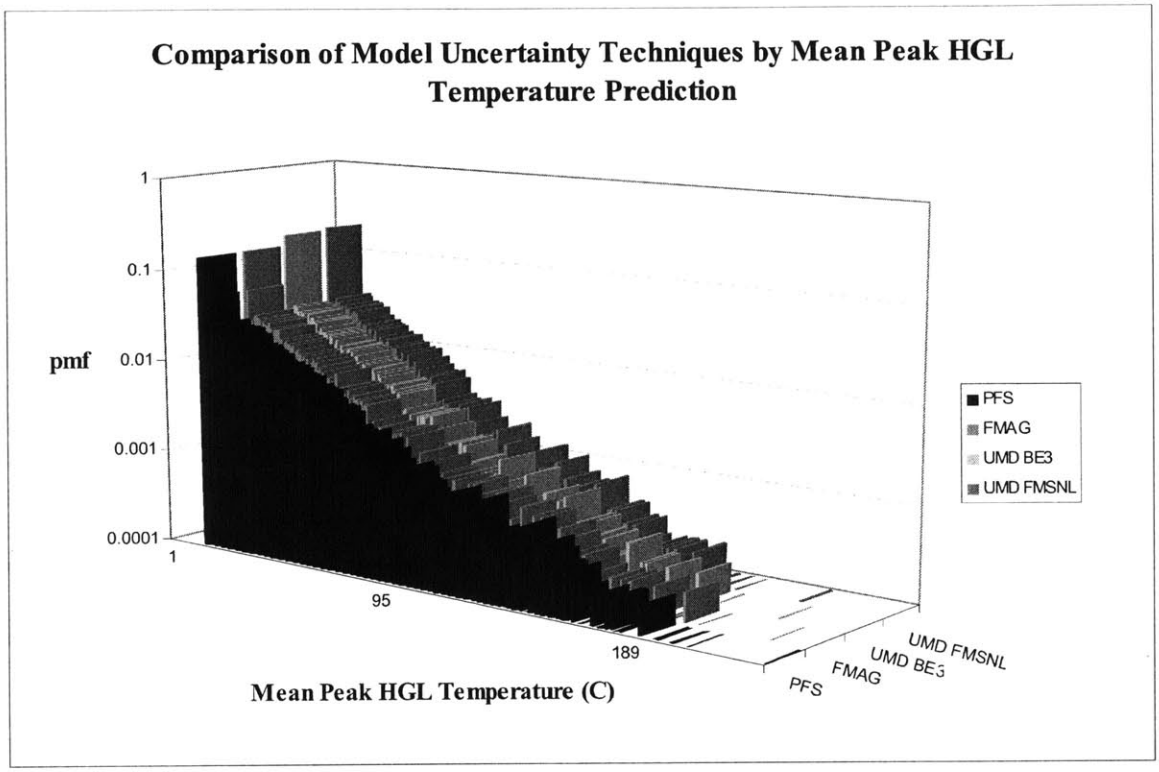

Figure 7-1: Comparison of Model Uncertainty Techniques by Mean Peak HGL Temperature

Although CFAST generally over-predicts peak HGL temperature, evaluating the probability that operators will be forced to abandon the MCR from the mean predictions alone is insufficient. Limiting our analysis in this way neglects the variance in the model uncertainty techniques that allows for the possibility that a real value, X, may exceed a model prediction, X_m.

To generate a cumulative probability of exceeding our abandonment threshold, it was necessary to consider the sum of the contributions from each simulation and normalize the result for our sample size, such that:

$$CDF = \Pr(T_{HGL}^{true} > 95C) = \frac{\sum_{i=1}^{10000} \Pr(T_{HGL}^{true} > 95C \mid X_{m,i})}{10000}$$

Ordering our model predictions by ascending peak HGL temperature, the model uncertainty techniques are compared by cumulative probability of exceeding the abandonment threshold in Figure 7-2.

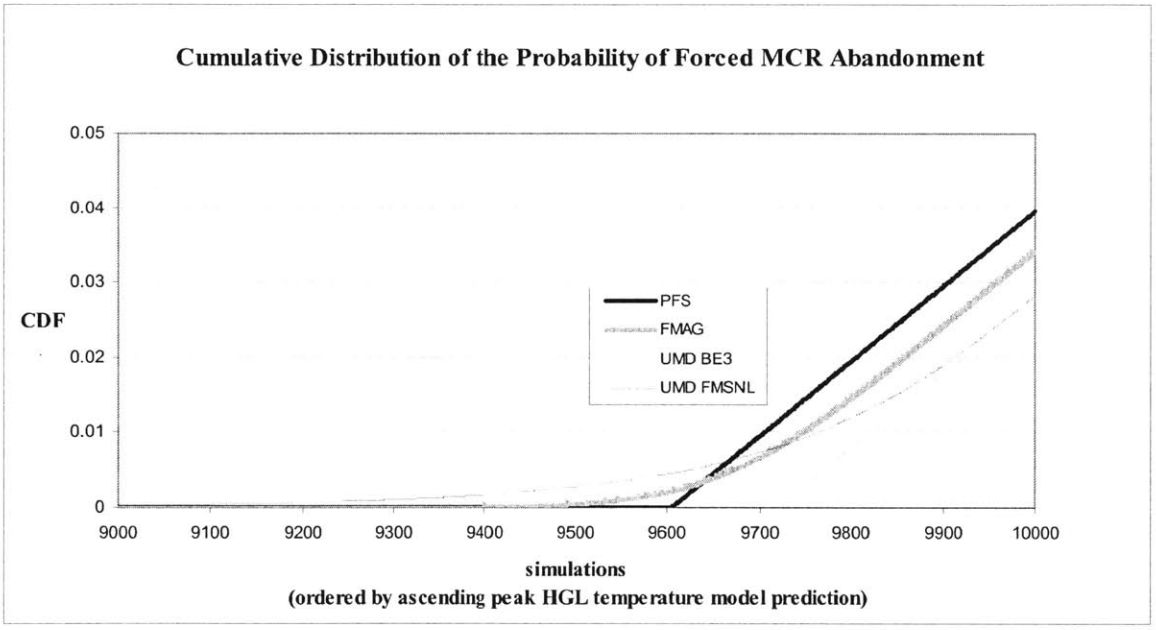

Figure 7-2: CDF of Forced MCR Abandonment

It is apparent from Figures 7-1 and 7-2 that the most conservative method of analyzing our scenario is to neglect model uncertainty altogether and use the values predicted by CFAST (PFS). Less conservative results can be obtained by using the method presented in the FMAG, with the UMD method yielding the least conservative results.

Although re-analyzing the UMD method with the inclusion of the FMSNL test 21 and 22 data caused a greater variance in the expected value of interest, the aggregate

effect of this difference is nearly negligible when a cumulative probability of exceedance is calculated (Figure 7-3).

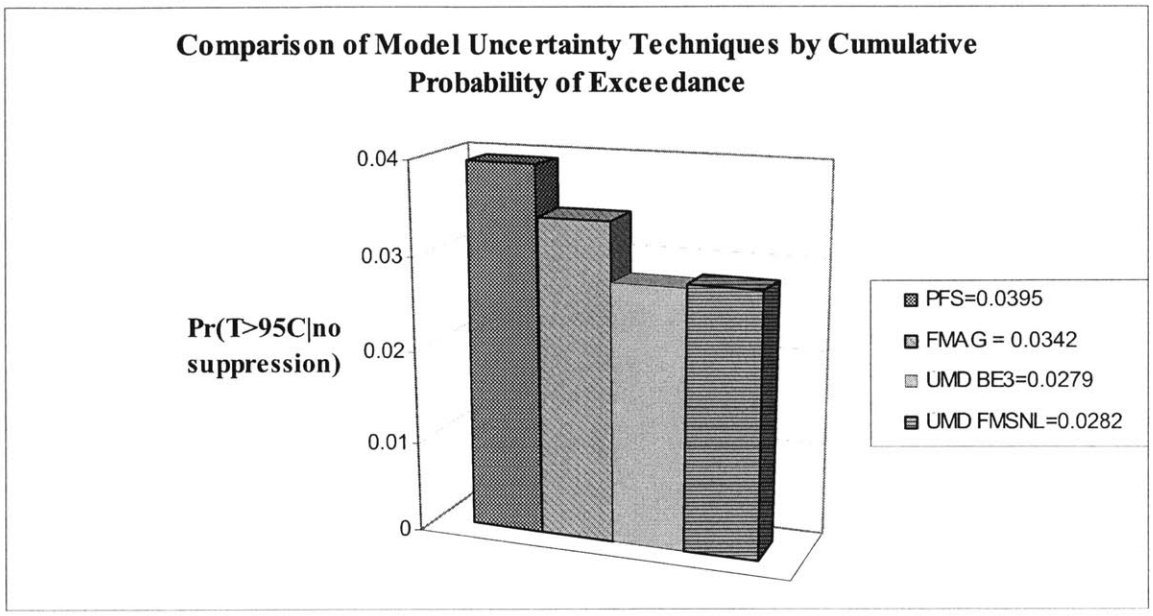

Figure 7- 3: Comparison of Model Uncertainty Techniques by Probability of Exceedance

Rather than constrain our analysis to one of the above techniques as we move forward, comparative results will be offered. However, because of the close agreement in the UMD methods their results will be considered as one.

While we are closer to assessing the probability that operators will be forced to abandon the MCR and take actions from the RSP in case of fire in benchboard 1-1, our results are still conservative in that no credit has been taken for manual fire suppression efforts. In Section VIII we will take operator suppression efforts into consideration as we refine our estimate of the probability of forced operator abandonment of the MCR.

VIII. FIRE SUPPRESSION ANALYSIS

In order for the scenario we are considering to take place a fire must cause the MCR to be abandoned. To this point we have only considered whether a fire *could* cause an abandonment condition, in this section we consider whether a fire *will* cause an abandonment condition.

In evaluating the combined model and parameter uncertainties present in our scenario, the goal was to develop an expression for the probability that a fire in benchboard 1-1 would force operator abandonment of the MCR if no suppression efforts were made. The final step in our fire growth and propagation analysis is to assess the probability that operators in the MCR will suppress a fire before an abandonment condition occurs. The probability of forced MCR abandonment is:

$$f_r = \Pr(T_{HGL} > 95C \mid Non-Suppression) * \Pr(Non-Suppression)$$

To ascertain the probability of non-suppression an event tree analysis will be conducted using the method presented in NUREG-6850 [2].

The MCR is a continuously occupied space with two heat detectors located on the ceiling such that once a fire is detected suppression efforts will begin immediately. However, there are no automatically actuated fixed suppression systems in the MCR.

In developing the event tree for our scenario, no credit was taken for prompt manual detection of the fire due to its location within a benchboard and the presence of a forced ventilation system that each contributes to likelihood that the operators will not detect the fire. It was also assumed that delayed manual detection was unnecessary due to the redundant heat detectors that will provide automatic detection with a negligible failure rate. The suppression event tree for our scenario is given in Figure 8-1.

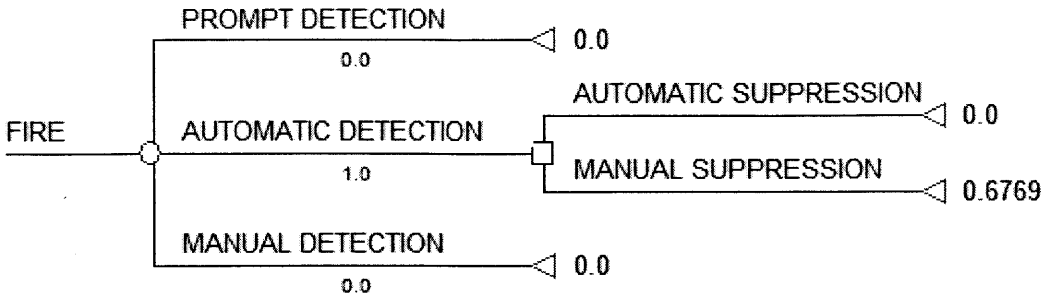

Figure 8-1: Fire Suppression Event Tree

Through an assessment of manual fire suppression historical data, generic industry-wide response rates (λ) for different plant locations have been developed to aid in the evaluation of the probability that a fire will be manually suppressed as a function of time. From the model presented in [2], the probability that a fire will not be suppressed is given as:

$$\Pr(NS) = e^{-\lambda_{MCR} * t_{SUPPRESSION}}$$

Where:

$\Pr(NS)$ = The probability of non-suppression.

$t_{SUPPRESSION} = t_{ABANDONMENT} - t_{DETECTION}$

$\lambda_{MCR} = 0.33\,\text{min}^{-1} = 0.0055 s^{-1}$

Finding the time available for suppression is done through analysis of the time series data generated in Section VI. Figure 8-2 is an example of how the time available for detection is obtained using the FMSNL 21 test case as an example.

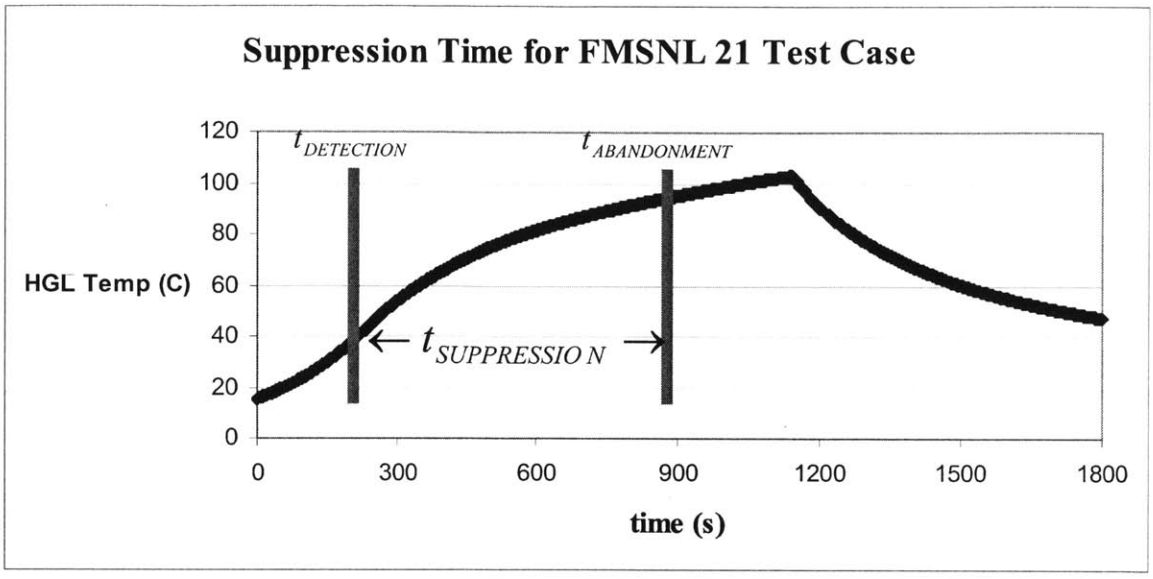

Figure 8-2: FMSNL Time Available for Suppression

To develop an accurate estimate of the time available for suppression in our scenario, each of the Monte Carlo samples performed by PFS (Section VI) that predicted a peak HGL temperature greater than the abandonment criterion were considered. This suppression time data was used to generate Figure 8-3, which evaluates each sample for the probability of non-suppression.

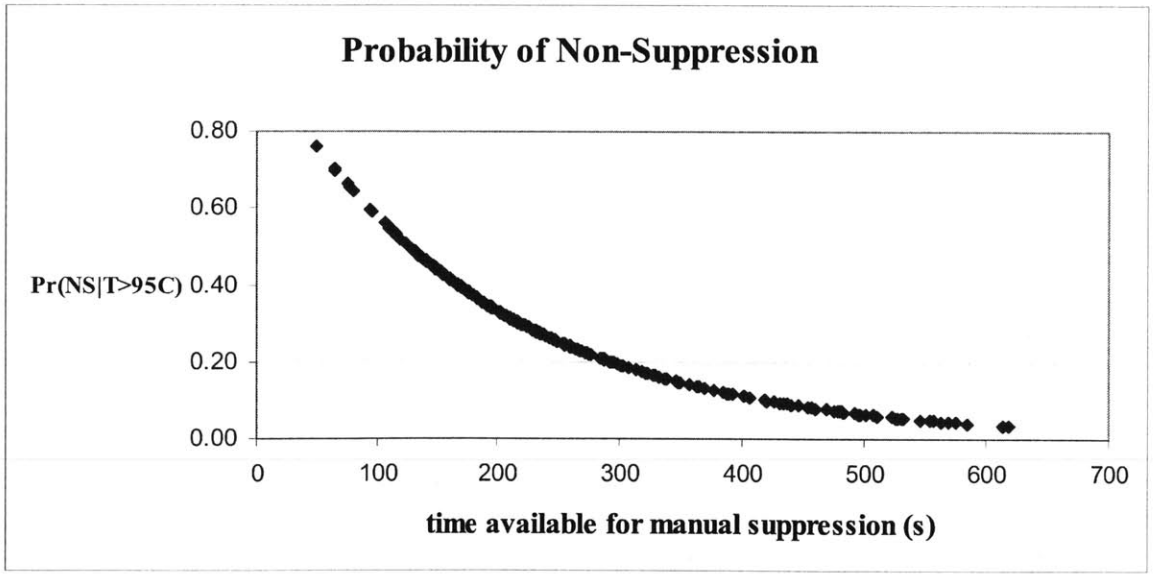

Figure 8-3: Probability of Non-Suppression

Once the probability of non-suppression of each scenario is known, the mean is calculated as:

$$\overline{\Pr(NS)} = \frac{\sum_{i=1}^{395} \Pr(NS)_i}{395} = 0.3231$$

We can now estimate the mean probability of operator abandonment of the MCR due to HGL temperature from a fire in benchboard 1-1 for each of our model uncertainty techniques as:

f_r^{PFS} = 0.0127

f_r^{FMAG} = 0.0111

f_r^{UMD} = 0.0091

This is a substantially lower estimate than that provided in NUREG-1150 [4] which gives the probability of operator abandonment of the MCR as Maximum Entropy distribution characterized by a lower bound of a = 0.01, an upper bound of b = 0.25, and a mean of $\mu = 0.1$ such that the probability density function (pdf) is given by [21]:

$$f(\theta \mid a, b, \mu) = \frac{\beta e^{\beta\theta}}{e^{\beta b} - e^{\beta a}}$$

Where $\beta(\beta \neq 0)$ satisfies:

$$\mu = \frac{be^{\beta b} - ae^{\beta a}}{e^{\beta b} - e^{\beta a}} - \frac{1}{\beta}$$

This results in the distribution given in Figure 8-4.

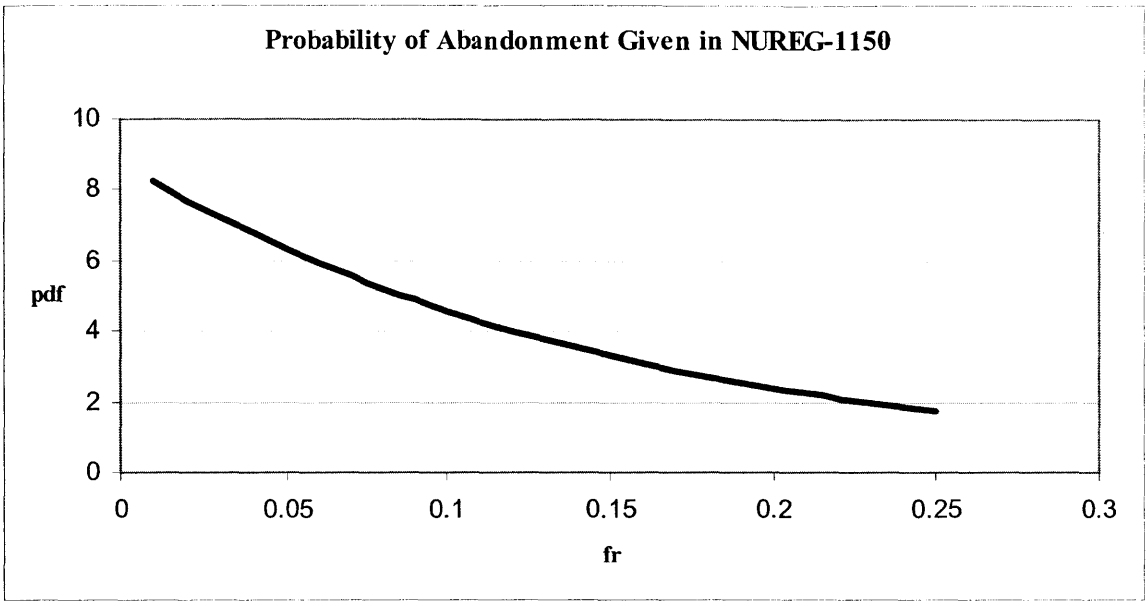

Figure 8-4: MCR Abandonment Probability Given in NUREG-1150

MCR abandonment probability has been an issue of great contention in the Fire PRA community. Application of state-of-the-art methods in estimating the probability of operator abandonment in this scenario suggest that the value given in NUREG-1150 is overly conservative; however, the value is still significant and MCR abandonment scenarios should not be automatically eliminated from consideration when conducting a fire PRA.

In Section X we will consider factors within an operator's control to mitigate the probability of a MCR abandonment scenario occurring.

Once operators are forced to abandon the MCR they are required to take actions from the RSP to prevent core damage. The probability of successful operator action will be considered in the next section.

IX. HUMAN RELIABILITY ANALYSIS

After the fire in benchboard 1-1 causes spurious actuation of a PORV and the operators are forced to abandon the MCR and station themselves at the RSP, they must shut the PORV block valve to prevent core damage. A low probability of successful operator action is expected due to the PORV closure status not being displayed on the RSP and the PORV block valve controls on the RSP not being electrically independent of the MCR benchboard where the fire is occurring.

NUREG-1921, *EPRI RES Fire Human Reliability Analysis Guidelines* [12], is currently a draft for public comment that provides guidance on estimating Human Error Probabilities (HEPs) for Human Failure Events (HFEs). Three general methods are given for analyzing post-fire human error probability:

(1) Screening HRA Quantification

(2) Scoping HRA Quantification

(3) Detailed HRA Quantification

These methods are sequentially less conservative and more detailed.

The screening method is the simplest and most conservative of the methods and is often used as a first step in determining which sequences warrant further consideration. The scoping method is less conservative than the screening method and uses decision tree logic to assign appropriate HEPs. Detailed HEP quantification can be accomplished through the use of the EPRI HRA CALCULATOR [25] or NUREG-1880, *A Technique for Human Event Analysis (ATHEANA)* [26]. Both of the detailed quantification methods require in-depth analysis of plant specific training information and procedures that are beyond the scope of this generalized report.

The screening method of quantifying HEPs has a specific category assigned to assess the actions taken subsequent to the abandonment of the MCR. For these actions a global screening value of 1.0 is assigned. It is acknowledged that this is a conservative estimate and that more detailed analysis should be performed for MCR abandonment scenarios.

The scoping method introduced in NUREG-1921 offers a method of performing a less conservative, but still simplified, analysis by taking into account how specific aspects of the fire scenario determine operator performance. Using the decision-tree format presented in NUREG-1921, it becomes immediately apparent that not having PORV indication available at the RSP is problematic. For our scenario, the scoping HRA decision tree simplifies to Figure 9-1.

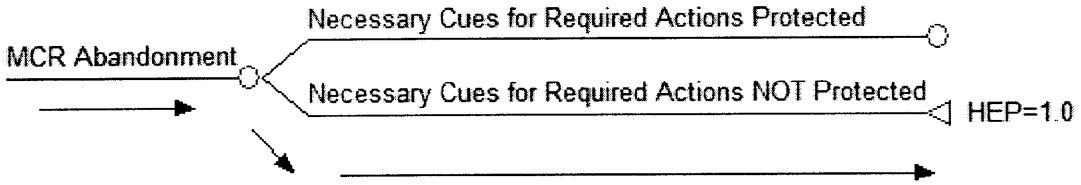

Figure 9-1: Scoping HRA Analysis for MCR Abandonment Scenario

Individual plants that show susceptibility to MCR abandonment scenarios may be able to obtain less conservative results using one of the detailed analysis techniques presented in NUREG-1921. However, for this scenario, the absence of a cue to alert the operators that a PORV is open and the further complication caused by not having the PORV block valve controls on the RSP electrically independent of the MCR benchboard make it difficult to justify taking credit for successful operator action after abandoning the MCR.

The results presented in NUREG-1150 do not offer a methodology for obtaining the probability that operators will successfully recover the plant from the RSP, which requires closing the PORV block valve. The value is given in the NUREG-1150 analysis as a Maximum Entropy distribution characterized by a lower bound of a = 0.0074, an upper bound of b = 0.74, and a mean of μ = .074 such that the probability density function (pdf) is given by [21]:

$$f(\theta \mid a, b, \mu) = \frac{\beta e^{\beta\theta}}{e^{\beta b} - e^{\beta a}}$$

Where $\beta(\beta \neq 0)$ satisfies:

$$\mu = \frac{be^{\beta b} - ae^{\beta a}}{e^{\beta b} - e^{\beta a}} - \frac{1}{\beta}$$

resulting in the distribution given in Figure 9-2.

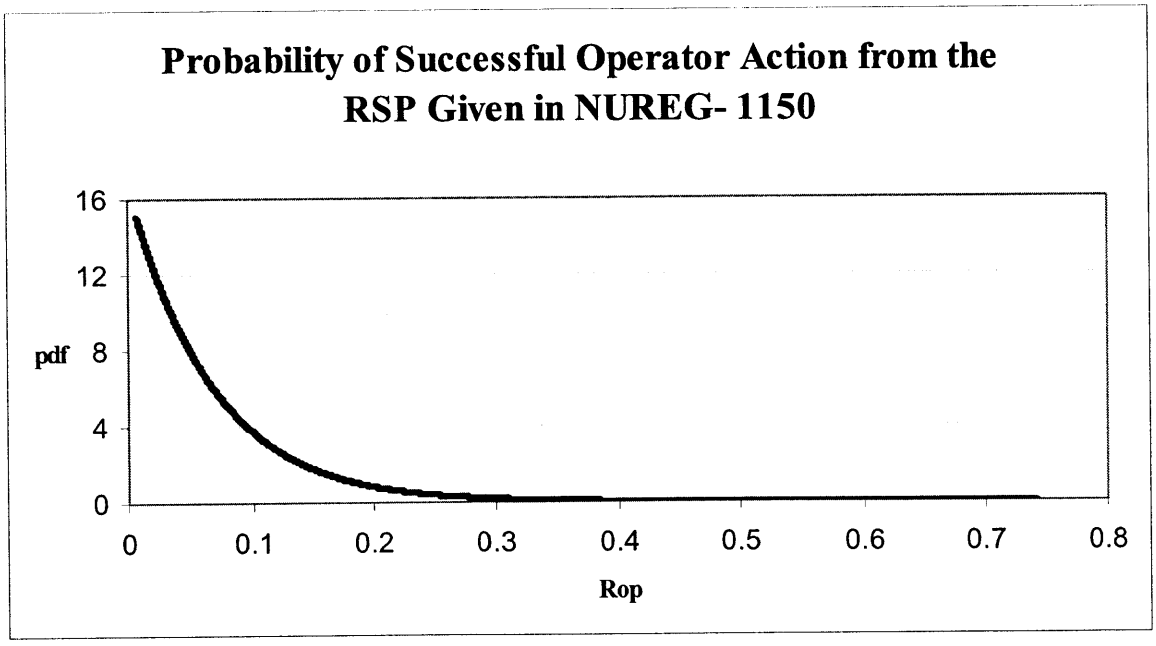

Figure 9-2: Probability of Successful Operator Action from the RSP Given in NUREG-1150

Although not taking credit for operator actions after forced abandonment of the MCR revises the total CDF estimate for this scenario upward, the combined effects of reduced fire ignition frequency and probability of MCR abandonment cause our updated distribution of CDF for this scenario to be significantly less than the values predicted in the NUREG-1150 analysis. These results, along with a discussion of the most important input parameters, will be presented in Section X.

X. CONCLUSIONS AND SENSITIVITY ANALYSIS

The final steps in our analysis are to combine the uncertainties from each step in our scenario to develop an updated CDF distribution that takes into account the interdependencies between the input parameters and to identify the factors that have the strongest influence on the final results.

In order to obtain an overall CDF distribution it is necessary to sample from the distributions of the individual factors obtained in the previous sections. From Section II, the resulting combined CDF is calculated as:

$$CDF = \lambda_{MCR} * f_a * f_r * R_{op}$$

Where:

CDF = The fire-induced core damage frequency for the MCR.

λ_{cr} = The frequency of MCR fires.

f_a = The area ratio of benchboard 1-1 to total cabinet area within the MCR.

f_r = The probability that operators will not successfully extinguish the fire before forced abandonment of the MCR.

R_{op} = The probability that operators will unsuccessfully recover the plant from the RSP. To successfully recover the plant, the operator must shut the PORV block valve, despite not having indication on the RSP that the PORV has lifted.

The resulting combined CDF distribution is given in Figure 10-1.

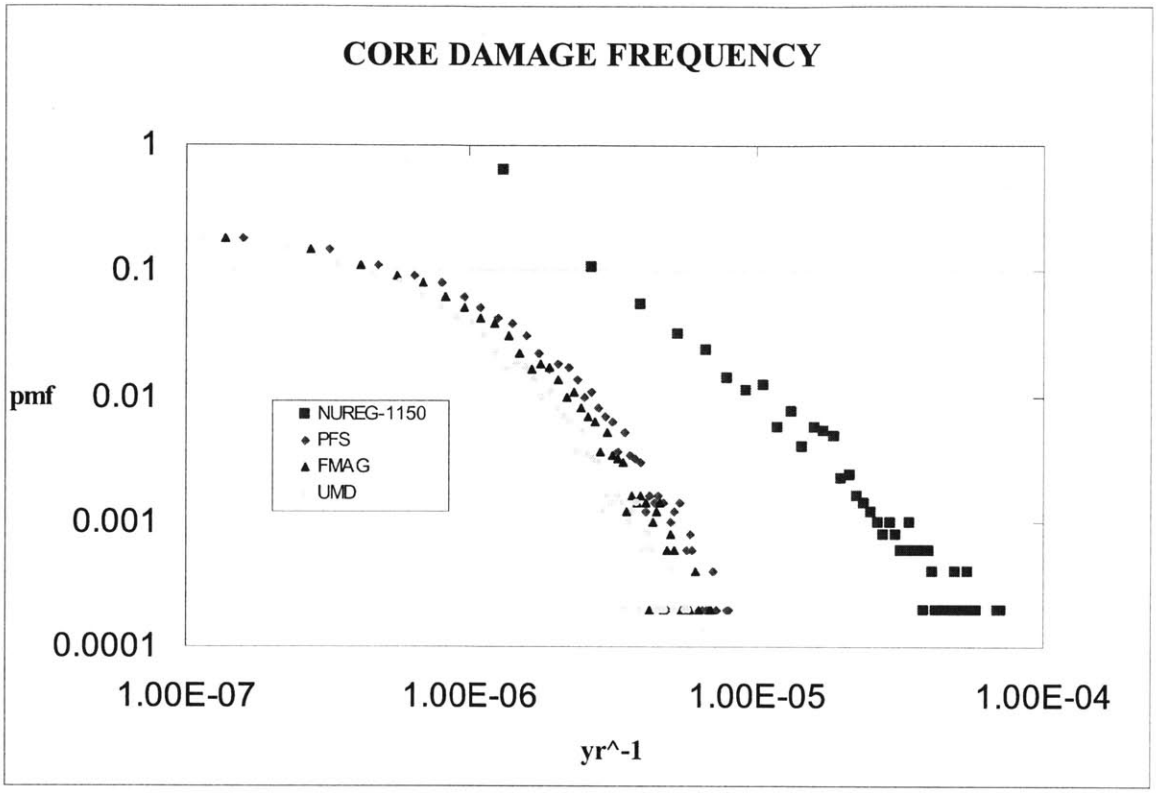

Figure 10-1: Comparison of CDF Distributions

Despite the inability to take credit for operator actions after forced abandonment of the MCR, each of the current methods used in this study shows that a reduction by a factor of approximately two in the mean value of the total CDF calculated in NUREG-1150 is expected. This is shown in Table 10-1.

CORE DAMAGE FREQUENCY (1/yr)		
METHOD	**MEAN**	**95th PERCENTILE**
NUREG-1150	1.58×10^{-6}	1.98×10^{-5}
PFS	9.61×10^{-7}	2.67×10^{-6}
FMAG	8.33×10^{-7}	2.33×10^{-6}
UMD	6.88×10^{-7}	1.92×10^{-6}

Table 10-1: Comparison of CDF by Method

Although current analysis methods indicate an overall reduction in the mean value of core damage frequency, the differences in the HEP quantification results between NUREG-1150 and NUREG-1921 obscure a dramatic decrease in the expected probability of a fire in benchboard 1-1 forcing MCR abandonment. By neglecting the R_{op} term our core damage frequency equation reduces to the probability of operator abandonment of the MCR due to a fire in benchboard 1-1, such that:

$$\Pr(abandonment) = \lambda_{MCR} * f_a * f_r$$

Where:

λ_{cr} = The frequency of MCR fires.

f_a = The area ratio of benchboard 1-1 to total cabinet area within the MCR.

f_r = The probability that operators will not successfully extinguish the fire before forced abandonment of the MCR.

Each of the current methods used to calculate the probability of forced MCR abandonment from a fire in benchboard 1-1 results in a reduction by a factor of approximately 20 in the mean value of the probability of forced MCR abandonment calculated in NUREG-1150. This is shown in Table 10-2 and Figure 10-2.

MCR ABANDONMENT PROBABILITY		
METHOD	**MEAN**	**95th PERCENTILE**
NUREG-1150	1.76×10^{-6}	7.36×10^{-5}
PFS	9.61×10^{-7}	2.67×10^{-6}
FMAG	8.33×10^{-7}	2.33×10^{-6}
UMD	6.88×10^{-7}	1.92×10^{-6}

Table 10-2: Comparison of MCR Abandonment Probability by Method

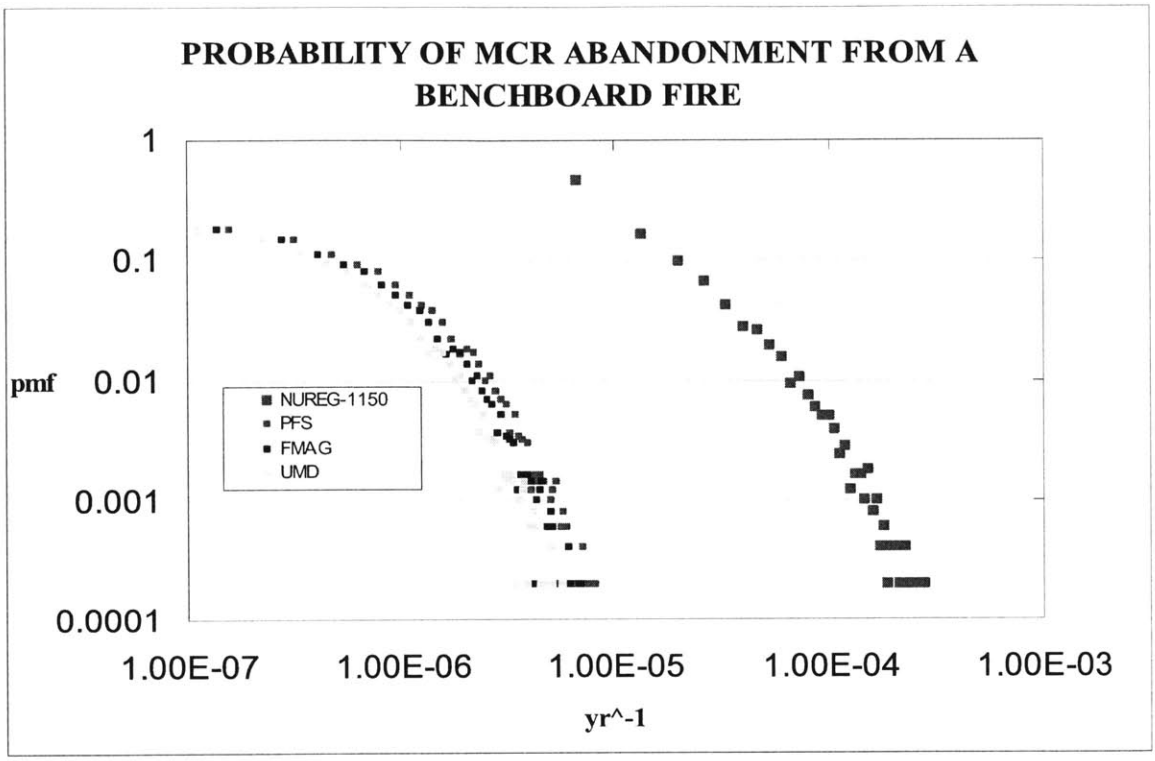

Figure 10-2: Comparison of MCR Abandonment Distributions

Although the frequency of fires causing MCR abandonment is much lower than previously assessed, it is still a significant contributor to total CDF and would not be eliminated in the screening process of a fire PRA.

In order to determine which input parameters have the strongest influence on the results of our fire model, PFS uses the Spearman Rank-order Correlation Coefficient (RCC) [15] to assess the sensitivity of an output value, Y, to an input parameter X. The RCC is defined as:

$$RCC = 1 - \frac{6\sum d_i^2}{n(n^2 - 1)}$$

Where:

$d_i = x_i - y_i$ = The difference between ranks of each observation.

n = The number of data pairs.

RCC measures the degree of monotonicity between input parameters and the chosen output, increasing in magnitude to a value of unity as input and output values approach perfect monotone functions of each other. A positive value of RCC indicates that as X increases, Y tends to increase. A negative value of RCC indicates that as X increases, Y tends to decrease.

RCC replaces raw scores with their associated ranks to reduce the effects of nonlinear data [27]. Therefore, RCC is independent of the distribution of the input parameters and allows the simultaneous identification of both modeling parameters and MCR properties that have the strongest influence on the peak HGL temperature achieved during our scenario [10].

The sensitivity of peak HGL temperature to the input parameters varied in Table 6-1 is shown in Figure 10-3. As expected [9], HRR has the most direct effect on peak HGL temperature, with HRR growth time and ventilation rate also having significant effects. Thermal properties of the MCR are minor factors.

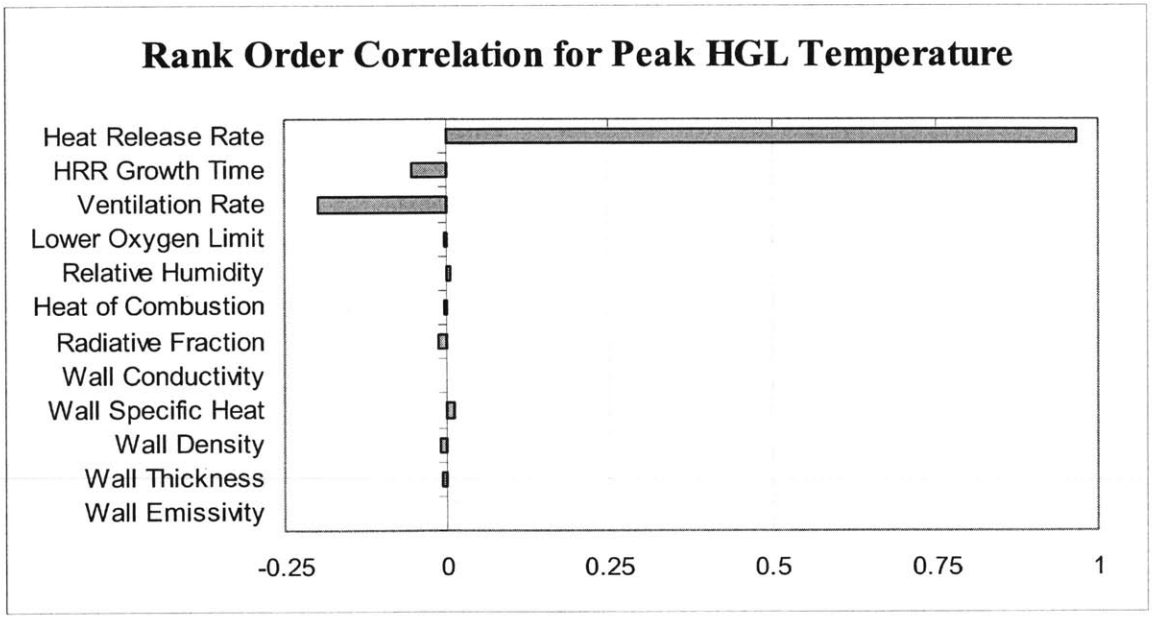

Figure 10-3: Rank Order Correlation Coefficient for Peak HGL Temperature

HRR and HRR growth time are modeling parameters that are out of the operator's control, whereas ventilation can be easily varied. Figure 10-4 illustrates how varying MCR ventilation rate for the FMSNL 21 test case modeled in Section IV affects the HGL temperature.

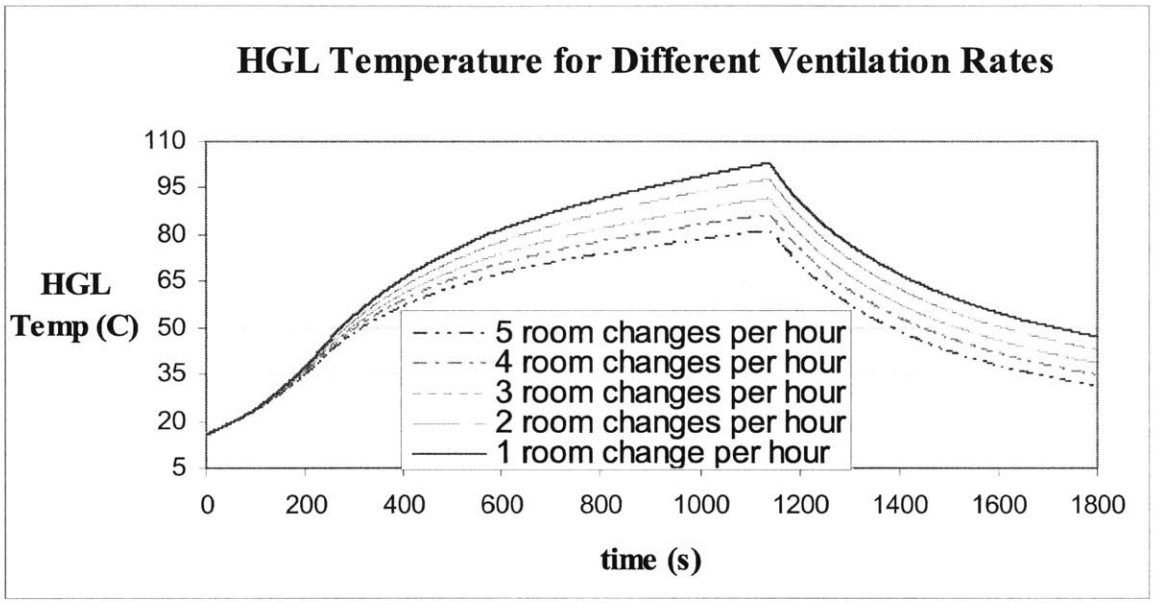

Figure 10-4: FMSNL 21 HGL Temperatures as a Function of Ventilation Rate

From Figure 10-4 it is apparent that a MCR abandonment condition due to exceeding the peak HGL temperature threshold will not be predicted by CFAST if the ventilation rate is increased from one to three room changes per hour in the FMSNL 21 test case.

The FMSNL 21 test case uses a HRR of 470 kW that is greater than 92% of expected fires. To find a ventilation rate that would more nearly preclude abandonment due to peak HGL temperature in a MCR identical to the FMSNL 21 test case, a limiting case simulation was conducted with a HRR of 702 kW (98^{th} percentile) and a minimal HRR growth time. In this extreme case, a ventilation rate of 10 room changes per hour

was sufficient to prevent the predicted peak HGL temperature from reaching the abandonment threshold of 95 °C.

In addition to our fire model, our analysis is sensitive to other factors. From the CDF equation introduced in Section II it is apparent that refinements of MCR fire ignition frequency estimates would have a linear effect on the estimate CDF. Also, the effect of increasing the rate at which fires are extinguished in the MCR (λ_{MCR}) would cause the mean probability of suppressing a fire that would otherwise cause MCR abandonment to increase. As an example, the effect of doubling the rate at which fires are extinguished increases the mean suppression probability by a factor of 1.29. This is shown in Figure 10-5.

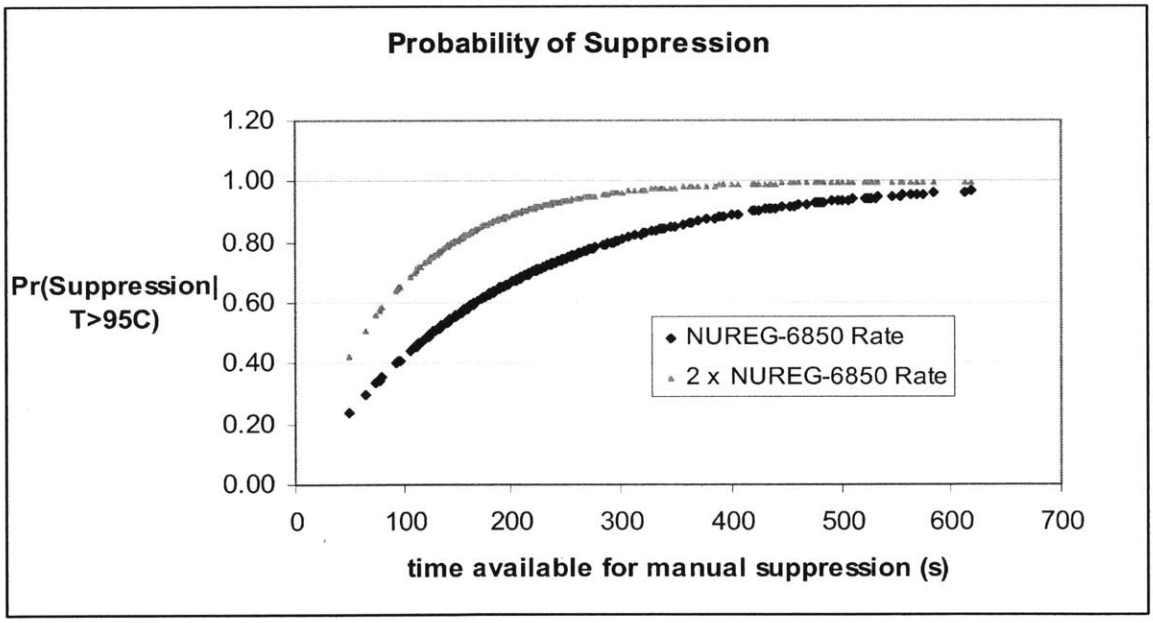

Figure 10-5: Effect of Doubling Fire Suppression Rate

Refinements in fire ignition frequency and fire suppression estimates are expected to revise the severity of this casualty downward as measures to prevent and suppress fires improve with time due to increased training and knowledge sharing practices.

The scoping method of quantifying the HEP introduced in NUREG-1921[12] is an adequate and conservative tool for our analysis. For our scenario, the design of the RSP is the primary factor leading to our conservative HEP estimate of 1.0. If proper indication were provided to operators once they were forced to abandon the MCR, and if their required actions did not involve operation of equipment not electrically independent of the fire, it is likely that the HEP estimate would be reduced by a factor of 2. However, this analysis would involve a review of plant specific procedures and time margins to core damage.

The results of our case study indicate that for existing plants the one controllable factor available to an operator to mitigate the probability of a MCR abandonment scenario is the MCR ventilation rate.

For plants yet to be constructed, the effects of a MCR casualty could be substantially reduced through an improved design of the RSP that provides the operators with the necessary cues and independent circuitry to take actions to terminate this casualty before core damage occurs.

The results of this study are heavily dependent on the distribution of HRR. The research into HRR distributions that is currently being conducted will help to provide regulators with the necessary tools to fully assess the contribution to core damage frequency from fires initiated from within the MCR.

It is important to note that this work is a limited study meant to apply to a specific scenario and may not be applicable to all scenarios, such as a complete loss of power or a fire in a vertical cabinet. PRA practitioners are encouraged to take note of the narrow range of applicability of the methods and results presented here.

REFERENCES

[1] NFPA 805, *Performance-Based Standard for Fire Protection for Light Water Reactor Electric Generating Plants*, National Fire Protection Association, Quincy, MA, 2001.

[2] *EPRI/NRC-RES Fire PRA Methodology for Nuclear Power Facilities: Volume 2: Detailed Methodology.* Electric Power Research Institute (EPRI), Palo Alto, CA, and U.S. Nuclear Regulatory Commission, Office of Nuclear Regulatory Research (RES), Rockville, MD: 2005, EPRI TR-1011989 and NUREG/CR-6850.

[3] *Nuclear Power Plant Fire Modeling Application Guide (NPP FIRE MAG),* U.S. Nuclear Regulatory Commission, Office of Nuclear Regulatory Research (RES), Rockville, MD, 2007, and Electric Power Research Institute (EPRI), Palo Alto, CA, NUREG-1934 and EPRI 1019195.

[4] "Severe Accident Risks: An Assessment for Five U.S. Nuclear Power Plants" NUREG-1150, December 1990.

[5] *Verification and Validation of Selected Fire Models for Nuclear Power Plant Applications ,Volume 1: Main Report,* U.S. Nuclear Regulatory Commission, Office of Nuclear Regulatory Research (RES), Rockville, MD, 2007, and Electric Power Research Institute (EPRI), Palo Alto, CA, NUREG-1824 and EPRI 1011999.

[6] Peacock, R.D., W.W. Jones, P.A. Reneke, and G.P. Forney, "Consolidated Model of Fire Growth and Smoke Transport (Version 6), User's Guide," SP 1041, National Institute of Standards and Technology, Gaithersburg, MD, 2005.

[7] Azarkhall, M., Ontiveros, V., Modarres, M., July 2009 "A Bayesian Framework for Model Uncertainty Considerations in Fire Simulation Codes" ICONE17-75684, Brussels, Belgium.

[8] Chavez, J.M.; Nowlen, S.P.; NUREG/CR-4527, SAND86-0336, Vol. 2, "A*n Experimental Investigation of Internally Ignited Fires in Nuclear Power Plant Control Cabinets Part II: Room Effects Tests*", U.S. Nuclear Regulatory Commission, Washington, DC, and Sandia National Laboratories, Albuquerque, NM, April 1987.

[9] *Verification and Validation of Selected Fire Models for Nuclear Power Plant Applications, Volume 5: Consolidated Fire and Smoke Transport Model (CFAST),* U.S. Nuclear Regulatory Commission, Office of Nuclear Regulatory Research (RES), Rockville, MD, 2007, and Electric Power Research Institute (EPRI), Palo Alto, CA, NUREG-1824 and EPRI 1011999.

[10] Hostikka, Simo and Keski-Rahkonen Olavi. *Probabilistic Simulation of Fire Scenarios, VTT* Building and Transport, PO Box 1803, FIN-02044 VTT, Finland, 2003.

[11] *Fire PRA Methods Enhancements: Additions, Clarifications, and Refinements to EPRI 1019189.* EPRI, Palo Alto, CA: 2008. 1016735.

[12] *EPRI/NRC-RES Fire Human Reliability Analysis Guidelines),* U.S. Nuclear Regulatory Commission, Office of Nuclear Regulatory Research (RES), Rockville, MD, 2007, and Electric Power Research Institute (EPRI), Palo Alto, CA, NUREG-1921 and EPRI 1019196.

[13] Saltelli, A., 'Sensitivity Analysis for Importance Assessment," *Risk Analysis, Vol. 22, 3, pp. 579-590.*

[14] Saltelli, A., Ratto, M., Andres, T., Campolongo, F., Cariboni, J., Gatelli, D., Saisana, M., Tarantola, S., Global Sensitivity Analysis: The Primer , 2008.

[15] C. Spearman, "The proof and measurement of association between two things" Amer. J. Psychol., 15 (1904) pp. 72–101.

[16] Meyer, S. P., July 2009 "Sources of Uncertainty in a Fire Probabilistic Safety Assessment" ICONE17-75360, Brussels, Belgium.

[17] "Analysis of Core Damage Frequency: Surry Power Station, Unit 1, External Events" NUREG/CR-4550, Vol. 3, Rev. 1, Part 3, December 1990.

[18] WCAP-16396-NP, "Westinghouse Owners Group Reactor Coolant Pump Seal Performance for Appendix R Assessments," Westinghouse Electric Co., January 2005.

[19] WCAP-17100-NP, "PRA Model for the Westinghouse Shut Down Seal" Westinghouse Electric Co., July 2009.

[20] Atwood, C.L. et al., 2003. Handbook of Parameter Estimation for Probabilistic Risk Assessment, NUREG/CR-6823, U. S. Nuclear Regulatory Commission, September 2003.

[21] Siu, N., and D. Kelly, 1998, Bayesian Parameter Estimation in Probabilistic Risk Assessment, in *Reliability Engineering and System Safety,* Vol. 62, pp. 89-116.

[22] Jones, W.W., R.D. Peacock, G.P. Forney, and P.A. Reneke, "Consolidated Model of Fire Growth and Smoke Transport (Version 6): Technical Reference Guide," NIST SP 1026, National Institute of Standards and Technology, Gaithersburg, MD, 2005.

[23] Heskestad, G., Delichatsios, M.A., 1977. *Environments of Fire Detectors. Phase 1. Effect of Fire Size, Ceiling Height and Materials. Vol. 2. Analysis*. NBS GCR 77-95, National Bureau of Standards. Gaithersburg, MD, 129 pp.

[24] Chapter 6; Section 3; NFPA HFPE-02; SFPE Handbook of Fire Protection Engineering. 3rd Edition, DiNenno, P. J.; Drysdale, D.; Beyler, C. L.; Walton, W. D., Editor(s), 3/171-188 p., 2002. Walton, W. D.; Thomas, P. H.

[25] Software Users Manual, *The Human Reliability Calculator Version 4.0*. EPRI, Palo Alto, CA, and Scientech, Tukwila, WA: January 2008. Product ID. 1015358.

[26] NUREG-1880, "ATHEANA User's Guide", Final Report, U.S. NRC, Washington, DC, June 2007.

[27] Hamby, D.M., *A Comparison of Sensitivity Analysis Techniques*, Health Phys. 1995 Feb; 68(2):195-204.

APPENDIX A: FMSNL INPUT FILE

```
VERSN,6,FM Test 21
!!
!!Environmental Keywords
!!
TIMES,1800,-50,0,10,1
EAMB,288.15,101300,0
TAMB,288.15,101300,0,50
CJET,WALLS
CHEMI,10,393.15
WIND,0,10,0.16
!!
!, !, Compartment keywords
COMPA,Compartment 1,18.3,12.2,6.1,0,0,0,MariniteFM,ConcreteFM,
MariniteFM
!!
!!vent keywords
!!
VVENT,2,1,1.08,2,1
MVENT,2,1,1,H,4.9,0.66,H,4.9,0.66,0.38,200,300,1
!!
!!fire keywords
!!
OBJECT,FMSNL_21,1,12,6.1,0,1,1,0,0,0,1
!!
,!,!target and detector keywords
DETECT,1,1,347.04,3.05,6.1,5.98,100,0,7E-05
DETECT,1,1,347.04,15.25,6.1,5.98,100,0,7E-05
TARGET,1,12,6.1,5.66,0,0,-1,TC,IMPLICIT,ODE
!!
!!misc. stuff
!!
THRMF,thermalfmsnl
```

APPENDIX B: FMSNL 21 INPUT TO CFAST-SCREEN VIEW

1. Simulation Environment

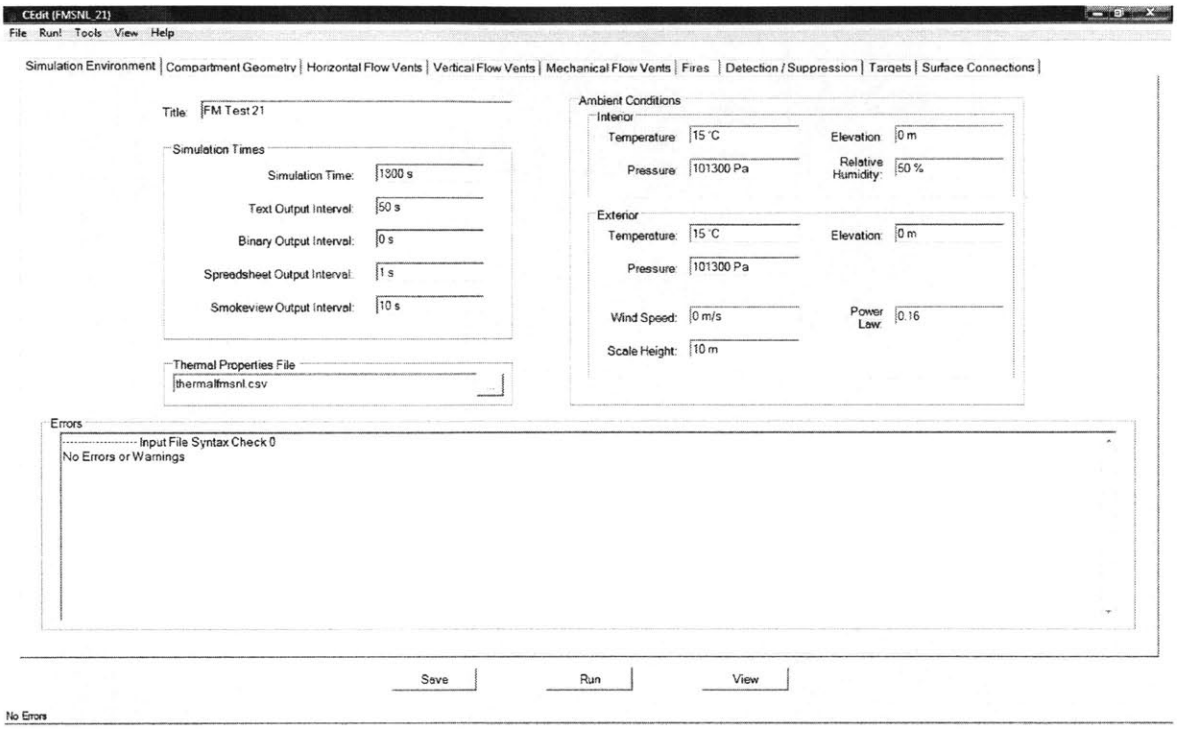

2. Compartment Geometry

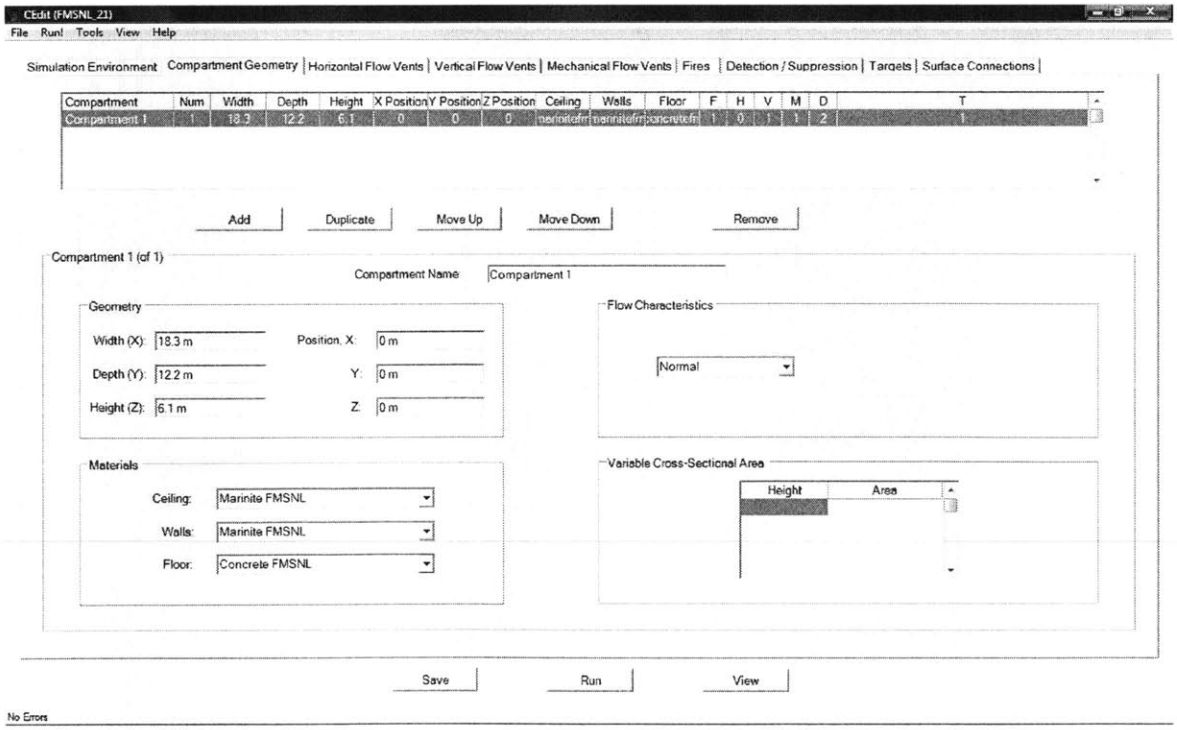

3. Horizontal Flow Vents

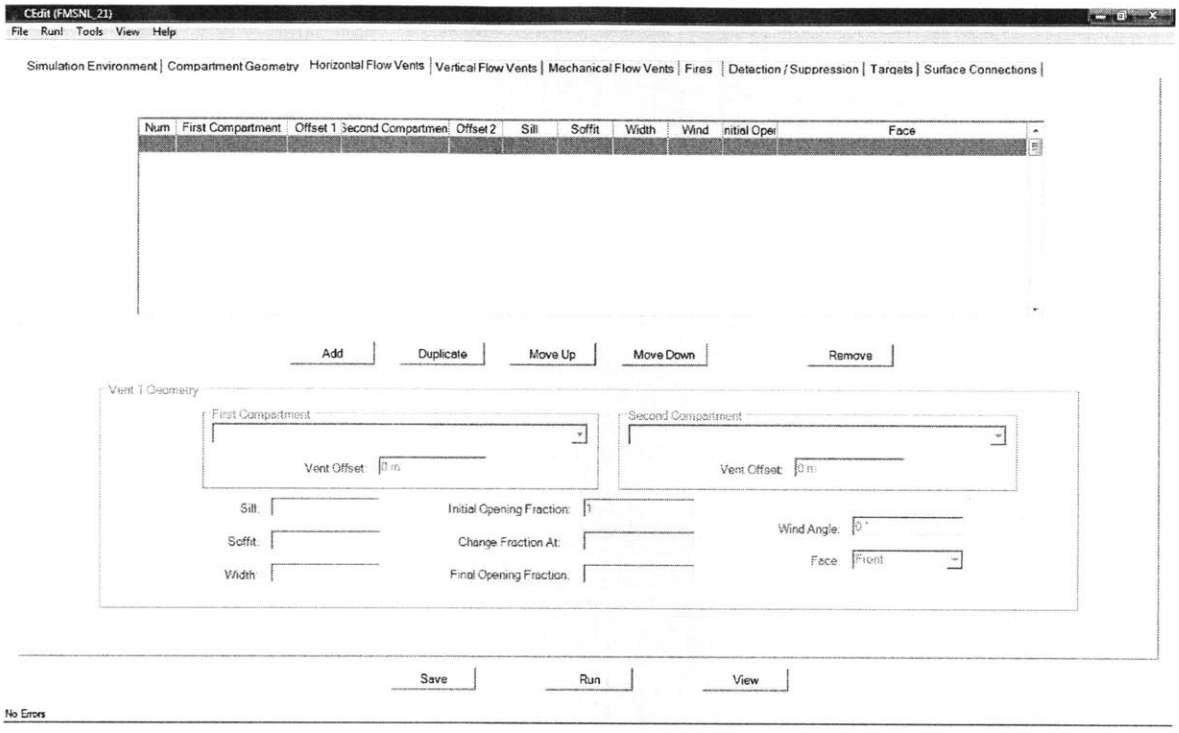

4. Vertical Flow Vents

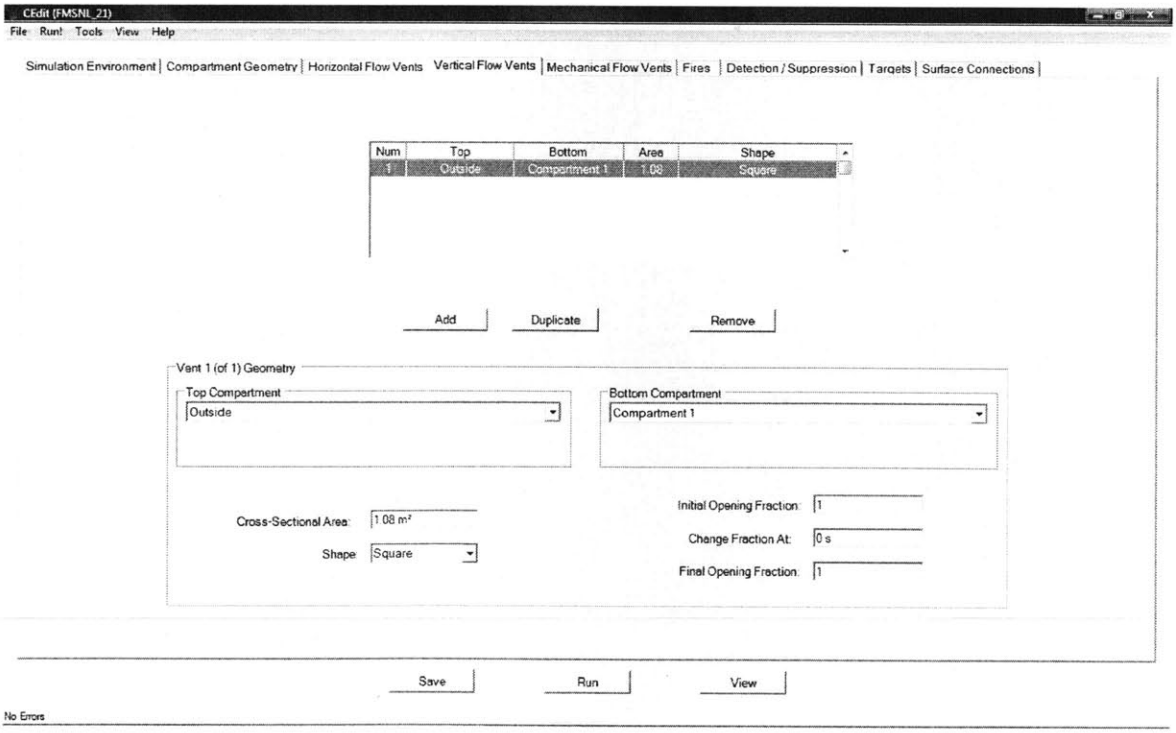

5. Mechanical Flow Vents

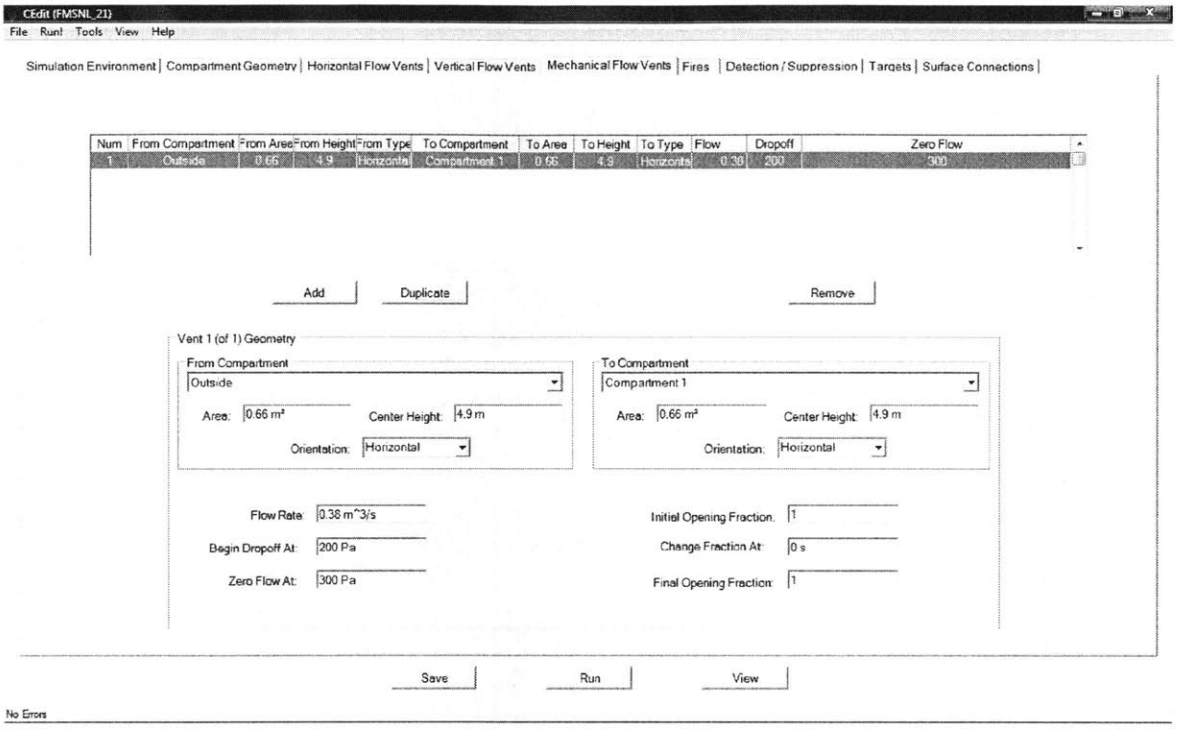

6. Fires

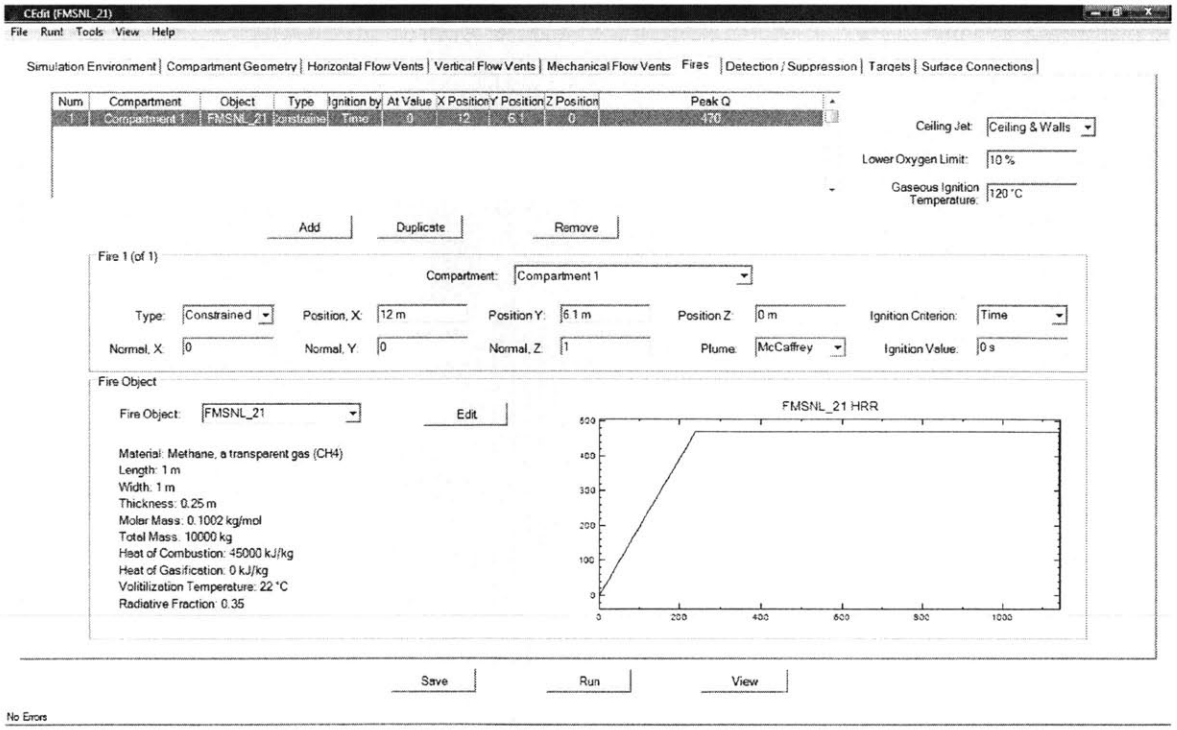

7. Detection/Suppression

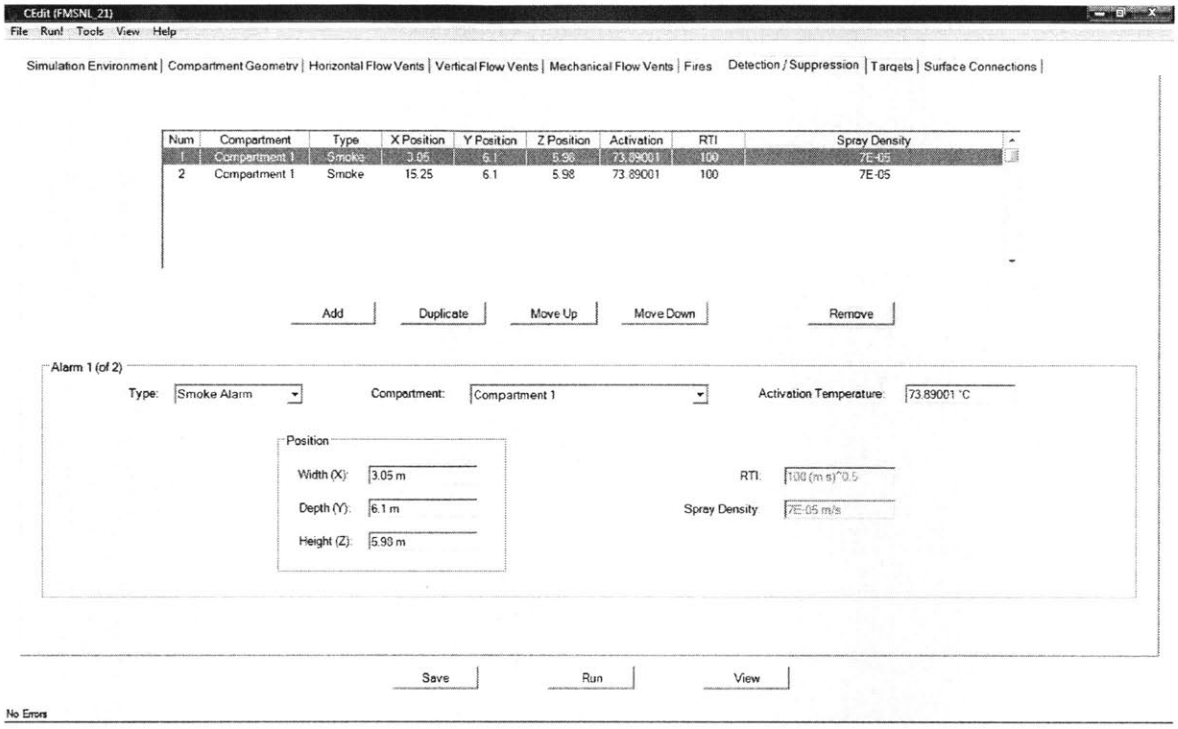

8. Targets

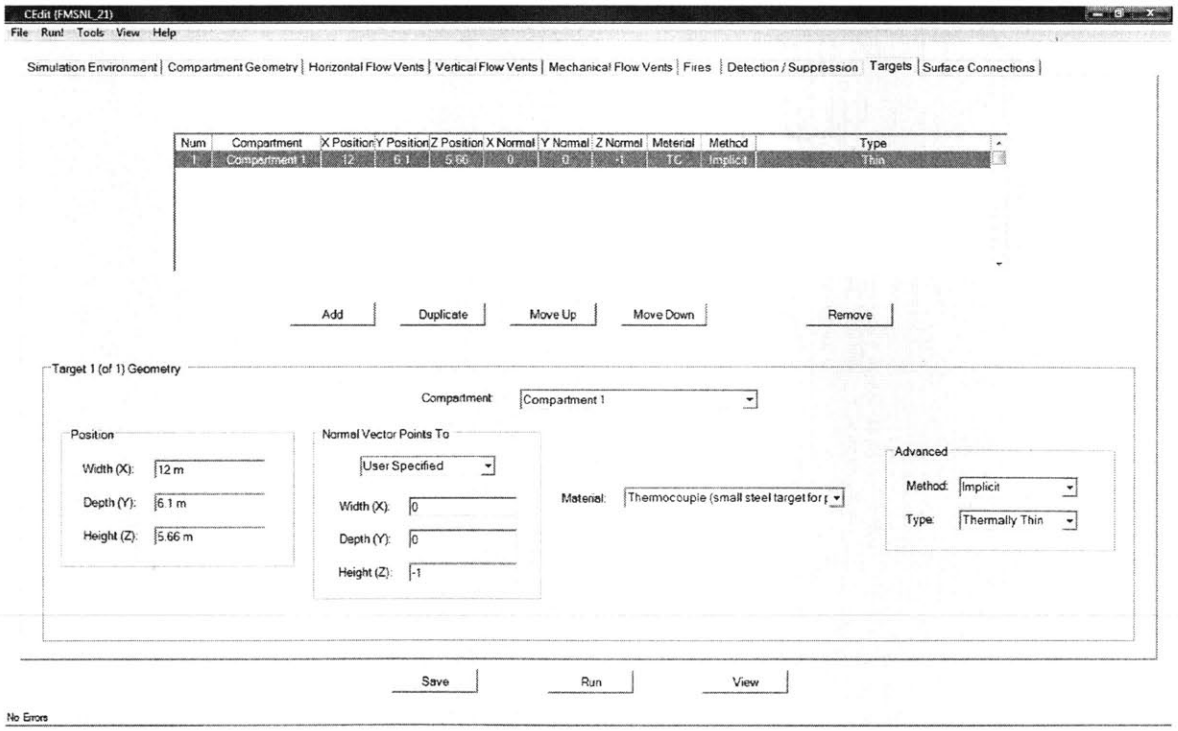

9. Surface Connections

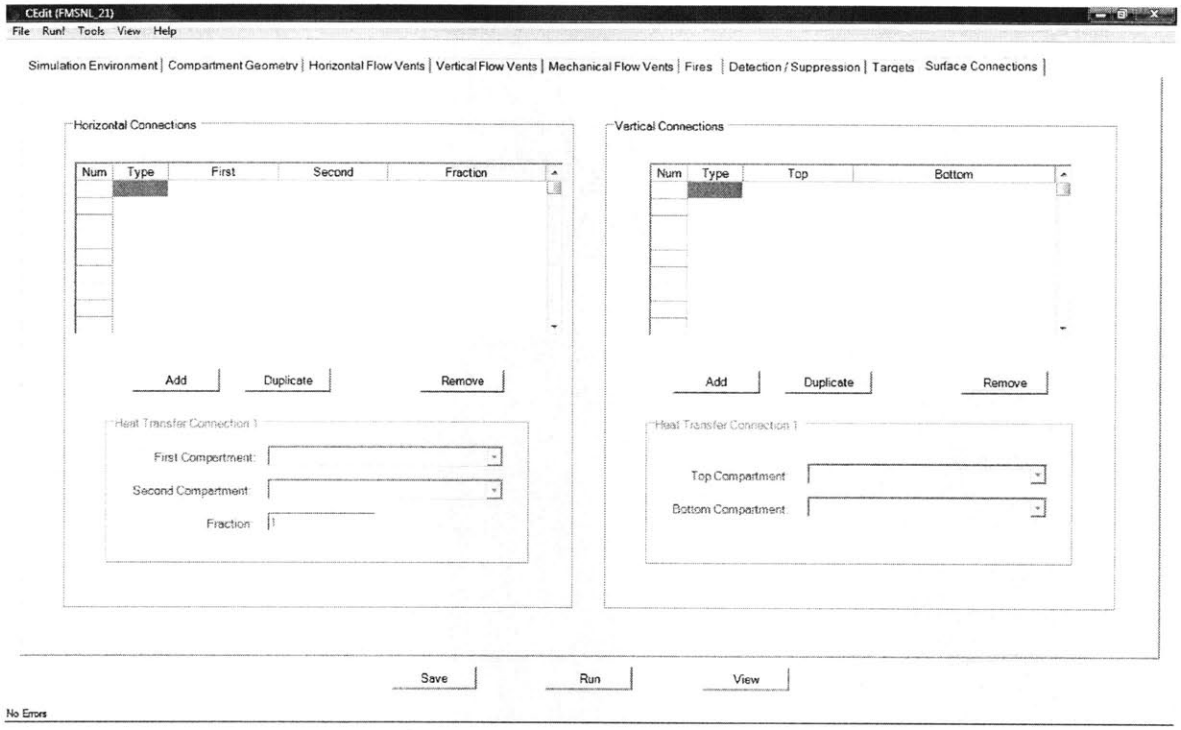

APPENDIX C: FMSNL THERMAL PROPERTIES INPUT FILE

Short Name	Conductivity	Specific Heat	Density	Thickness	Emissivity	HCl Coefficients	Long Name
METHANE	0.07	1090	930	0.0127	0.04	0	Methane, a transparent gas (CH4)
MineralBE2	0.2	150	500	0.05	0.95	0	Mineral Wool BE2
SteelBE2	54	425	7850	0.001	0.95	0	Steel ICFMP BE2
ConcreteBE2	2	900	2300	0.15	0.95	0	Concrete ICFMP BE2
MARIBE3	0.12	1250	737	0.0254	0.8	0	Marinite ICFMP BE3 (2 1/2 in layers)
GYPBE3	0.16	900	790	0.0254	0.9	0	Gypsum ICFMP BE3 (2 1/2 in layers)
XLP_C_BE3	0.21	1560	1375	0.01	0.95	0	F XPE Cable ICFMP BE3
PVC_C_BE3	0.147	1469	1380	0.01	0.95	0	PVC Slab ICFMP BE3
XLP_P_BE3	0.21	1560	1375	0.191	0.95	0	F XPE Cable ICFMP BE3
PVC_P_BE3	0.147	1469	1380	0.191	0.95	0	PVC Slab ICFMP BE3
SteelBE4	44.5	480	7743	0.02	0.95	0	Steel ICFMP BE4
ConcreteBE4	2.1	880	2400	0.25	0.95	0	Concrete ICFMP BE4 and BE5
LiteConcBE4	0.11	1350	420	0.3	0.95	0	Lightweight Concrete ICFMP BE4/BE5
PVC_P_BE4	0.134	1586	1380	0.015	0.8	0	PVC Power Cable BE4
PVC_C_BE4	0.134	1586	1380	0.007	0.8	0	PVC Control Cable BE4
MariniteFM	0.12	1250	720	0.025	0.95	0	Marinite FMSNL
ConcreteFM	1.8	1040	2280	0.15	0.95	0	Concrete FMSNL
FireBrickNBS	0.36	1040	750	0.113	0.8	0	Fire Brick NBS
CeramicNBS	0.09	1040	128	0.05	0.97	0	Ceramic Fiber NBS
MariniteNBS	0.12	1250	720	0.0127	0.83	0	Marinite NBS
GypsumNBS	0.17	1090	930	0.0127	0.95	0	Gypsum NBS
ConcreteNBS	1.8	1040	2280	0.102	0.95	0	Concrete NBS
TC	54	425	7850	0.001	0.95	0	Thermocouple (small steel target for plume temp)

APPENDIX D: WINBUGS INPUT FILE FOR HGL DATA (BE3 ONLY)

```
bm~dunif(-10,10)
sm~ dunif(0,10)
taum<-1/pow(sm,2)
pe<-0.08

be<-(log(1+pe)+log(1-pe))/2
se<-(log(1+pe)-log(1-pe))/(2*1.95996398454005)

bt<-bm-be
st<-sqrt(pow(sm,2)+pow(se,2))

C <- 1000

 for( i in 1 : N )
        {zeros[i] <- 0
        L[i] <- pow(exp(-0.5*pow((log(x[i,2]/x[i,1])-
        bt)/st,2))/(sqrt(2*3.141592654)*st)/(x[i,2]/x[i,1]),x[i,3])
          ghr[i] <- ( -1) * log(L[i]) + C
        zeros[i] ~ dpois(ghr[i])}

fm~dlnorm(bm,taum)

logfm<-log(fm)
           for( j in 1 : 9 )
        {yy[j]<-xx[j]*fm
        P218[j]<-1-phi((log(218)-bm-log(xx[j]))/sm)
        P330[j]<-1-phi((log(330)-bm-log(xx[j]))/sm)}
```

APPENDIX E: WINBUGS INPUT FILE FOR HGL DATA (BE3 + FMSNL 21/22)

```
bm~dunif(-10,10)
sm~ dunif(0,10)
taum<-1/pow(sm,2)
pe<-0.08

be<-(log(1+pe)+log(1-pe))/2
se<-(log(1+pe)-log(1-pe))/(2*1.95996398454005)

bt<-bm-be
st<-sqrt(pow(sm,2)+pow(se,2))

C <- 1000

 for( i in 1 : N )
        {zeros[i] <- 0
        L[i] <- pow(exp(-0.5*pow((log(x[i,2]/x[i,1])-
        bt)/st,2))/(sqrt(2*3.141592654)*st)/(x[i,2]/x[i,1]),x[i,3])
          ghr[i] <- ( -1) * log(L[i]) + C
        zeros[i] ~ dpois(ghr[i])}

fm~dlnorm(bm,taum)

logfm<-log(fm)
           for( j in 1 : 9 )
        {yy[j]<-xx[j]*fm
        P218[j]<-1-phi((log(218)-bm-log(xx[j]))/sm)
        P330[j]<-1-phi((log(330)-bm-log(xx[j]))/sm)}
```

APPENDIX F: FMSNL 21 INPUT TO PFS

I. CFAST CONTROL

CFAST Model and Execution Control

PFS: Probabilistic Fire Simulator v4.0

VTT Technical Research Centre of Finland

Fire

Type	1	0 = constant, 1 = t2 + exp. de 2 = Flame front velocity 4 = Cable fire (Mangs)
RHR Growth time (s)	320	101-114 Household appl.
RHR limiter (kW)	470	201-205 Detector test fires
Decay rate (s)	10	301-306 NPP cabinets
Decay start (s)	1140	
MaxRHR (kW)	470.0	
Scaling factor	1	
Source height (m)	0	
RHR/fuel area	470	kW/m2

Ambient

Ambient temp	15	C
Ambient pres	1.013	bar

Sprinkler/Detector Control

Detector type	1	1=smoke, 2 = heat
Sprinkler	0	0 = detector, 1 = sprinkle
RTI	100	(ms)^(1/2)
Tact	73.89001	C

CFAST control

Cfast directory: C:\NIST\cfast511

Iteration control

	xval	nsteps	
DTCHECK	1.0E-09	100	
(default	1.0E-09	100)	
Nrows	101	18	dt output
CallMode	1		0 = normal 2 = save 1 = debug

Create thermal database

ThDbCreate: TRUE (default FALSE)

If thermal data is randomly sampled, choose TRUE. Otherwise use FALSE and existing thermal data base is used (faster).

II. CFAST INPUT

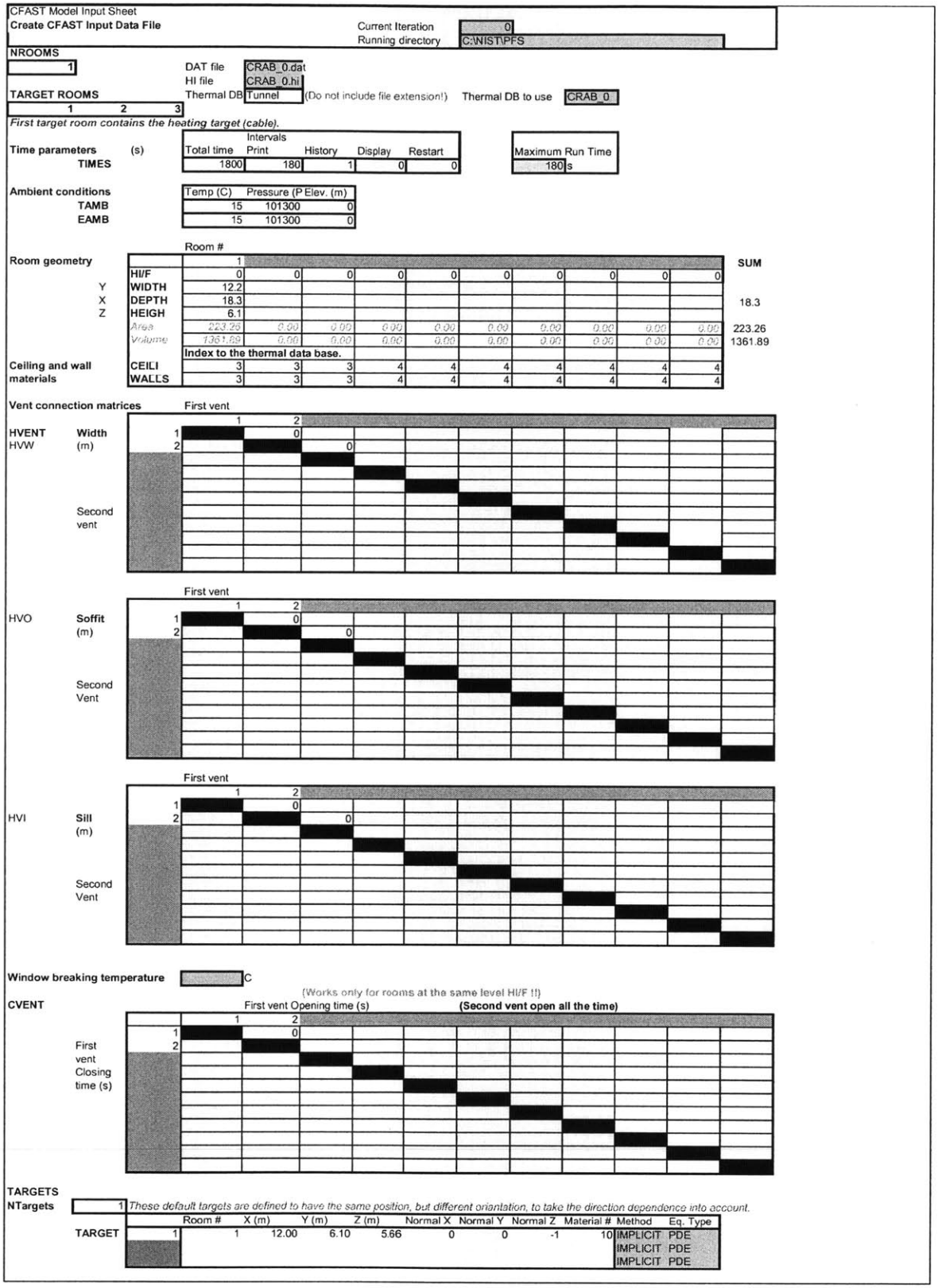

CFAST Model Input Sheet

Create CFAST Input Data File

Current Iteration: 0

Running directory: C:\NIST\PFS

NROOMS: 1

DAT file: CRAB_0.dat

HI file: CRAB_0.hi

TARGET ROOMS: 1 2 3

Thermal DB: Tunnel (Do not include file extension!)

Thermal DB to use: CRAB_0

First target room contains the heating target (cable).

Time parameters (s) — **TIMES**

Intervals				
Total time	Print	History	Display	Restart
1800	180	1	0	0

Maximum Run Time: 180 s

Ambient conditions

	Temp (C)	Pressure (P	Elev. (m)
TAMB	15	101300	0
EAMB	15	101300	0

Room geometry

		Room # 1	SUM
	HI/F	0	
Y	**WIDTH**	12.2	
X	**DEPTH**	18.3	18.3
Z	**HEIGH**	6.1	
	Area	223.26	223.26
	Volume	1361.89	1361.89
Ceiling and wall materials		Index to the thermal data base.	
	CEILI	3	
	WALLS	3	

Vent connection matrices

First vent

HVENT HVW — **Width** (m) — Second vent

	1	2
1	0	
2		0

First vent

HVO — **Soffit** (m) — Second Vent

	1	2
1	0	
2		0

First vent

HVI — **Sill** (m) — Second Vent

	1	2
1	0	
2		0

Window breaking temperature C

(Works only for rooms at the same level HI/F !!)

CVENT

First vent Opening time (s) **(Second vent open all the time)**

First vent Closing time (s)

	1	2
1	0	
2		0

TARGETS

NTargets: 1 *These default targets are defined to have the same position, but different orientation, to take the direction dependence into account.*

	Room #	X (m)	Y (m)	Z (m)	Normal X	Normal Y	Normal Z	Material #	Method	Eq. Type
TARGET 1	1	12.00	6.10	5.66	0	0	-1	10	IMPLICIT	PDE
									IMPLICIT	PDE
									IMPLICIT	PDE

DETECTORS

NDetectors 2 (1 for smoke, 2 for heat)

		Type	Room #	Tactiv (C)	X (m)	Y (m)	Z (m)	RTI (m.s)1	Sprinkler	Spray density (m/s)	
DETECT	1	1	1	73.89001	3.05	6.10	5.98	100	0	0	CAUTION! Don't use!
	2	1	1	73.89001	15.25	6.10	5.98	100	0	0	spray density > 0.0046 gives extiction, < 0.0046 nothing!!

FANS It is possible to define fans between the rooms, but not ductwork

Nfans 1 **MVOPN** 1 = Horizontal (in ceiling), 2 = vertical **MVFAN**

	1st room	Orientatiion	Height (m)	2nd room	Orientation	Height (m)	Area (m2)	Pmin (Pa)	Pmax (Pa)	Flow (m3/s)
1	1	1	4.900	2	1	4.900	0.66	0.00	300	0.38

FIRE SOURCE PROPERTIES

Chemistry

	Molar weig	Humidity (%)	LOI (%)	-DHc (J/kg)	T(fuel,init) K	T(ign, gas) K	Radiative fraction
CHEMI	16	50	10	4.50E+07	288.15	393.15	0.35

Compartment of fire origin

LFBO 1

Fire Type

LFBT 2 *1 = unconstrained fire, 2 = constrained*

Maximum Fire Area 1 m2

Fire height 0 m

Fire Position

	X (m)	Y (m)	Z (m)
FPOS	12	5.1	0

Ceiling jet OFF, CEILING, WALL, ALL

CJET ALL

Time series

	FTIME	FMASS	FHIGH	FAREA	FQDOT	Specie1 OD	Specie2 CO
0	0	0	0	1	0	0.01	0
1	90	0.001758	0	1	79101.56	0.01	0
2	180	0.007031	0	1	316406.3	0.01	0
3	270	0.010444	0	1	470000	0.01	0
4	360	0.010444	0	1	470000	0.01	0
5	450	0.010444	0	1	470000	0.01	0
6	540	0.010444	0	1	470000	0.01	0
7	630	0.010444	0	1	470000	0.01	0
8	720	0.010444	0	1	470000	0.01	0
9	810	0.010444	0	1	470000	0.01	0
10	900	0.010444	0	1	470000	0.01	0
11	990	0.010444	0	1	470000	0.01	0
12	1080	0.010444	0	1	470000	0.01	0
13	1170	0.001106	0	1	49787.07	0.01	0
14	1260	1.37E-07	0	1	6.144212	0.01	0
15	1350	1.69E-11	0	1	0.000758	0.01	0
16	1440	2.08E-15	0	1	9.36E-08	0.01	0
17	1530	2.57E-19	0	1	1.15E-11	0.01	0
18	1620	3.17E-23	0	1	1.43E-15	0.01	0
19	1710	3.91E-27	0	1	1.76E-19	0.01	0
20	1800	4.82E-31	0	1	2.17E-23	0.01	0

Possible species

HCN
HCL
HCR
CT
O2
OD
CO

APPENDIX G: STUDENT BIOGRAPHY

Lieutenant Mark Minton is originally from Northern California and enlisted in the United States Navy after graduating from Clayton Valley High School in 1995. After completing the Naval Nuclear Power School enlisted curriculum, he was selected for the Nuclear Enlisted Commissioning Program and ordered to Oregon State University, where he received a Bachelor of Science in Nuclear Engineering in 2001.

After being commissioned, he reported to USS SHOUP (DDG 86), where he served as Communications Officer and achieved qualification as a Surface Warfare Officer. He was subsequently ordered to return to Naval Nuclear Power School, this time to complete the officer curriculum.

Upon completion of Nuclear Power training, Lieutenant Minton reported to USS RONALD REAGAN (CVN 76) where he served in Reactor Department and achieved qualification as Nuclear Engineering Officer. He was subsequently selected for lateral transfer to the Engineering Duty Officer (Nuclear) community.

In 2008, Lieutenant Minton received a Master of Engineering Management from Old Dominion University.

Lieutenant Minton is currently pursuing a Nuclear Engineer's Degree and a Master of Science in Nuclear Science in Engineering at the Massachusetts Institute of Technology.

Upon completion of his studies at the Massachusetts Institute of Technology, Lieutenant Minton has been ordered to report to the Supervisor of Shipbuilding, Newport News, Virginia, where he will be assigned duties pertaining to the design, construction, conversion, and overhaul of nuclear powered aircraft carriers.